NASA TN D-1266

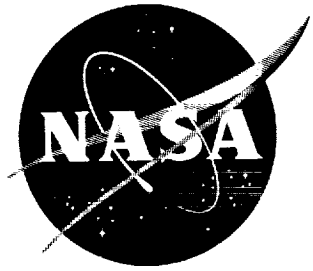

TECHNICAL NOTE

D-1266

INDUCED PRESSURES ON CYLINDRICAL RODS WITH VARIOUS NOSE DRAGS AND NOSE SHAPES AT MACH NUMBERS OF 17 AND 21

By Robert D. Witcofski and Arthur Henderson, Jr.

Langley Research Center
Langley Station, Hampton, Va.

NATIONAL AERONAUTICS AND SPACE ADMINISTRATION
WASHINGTON
May 1962

Q

NATIONAL AERONAUTICS AND SPACE ADMINISTRATION

TECHNICAL NOTE D-1266

INDUCED PRESSURES ON CYLINDRICAL RODS WITH VARIOUS NOSE DRAGS AND NOSE SHAPES AT MACH NUMBERS OF 17 AND 21

By Robert D. Witcofski and Arthur Henderson, Jr.

SUMMARY

A systematic investigation of induced pressures has been made at a free-stream Mach number of 17 and 21 in helium flow on six pairs of axially symmetric, flow-alined, cylindrical models in order to determine the range of validity of the nose-shape-independence concept of the blast-wave theory. Each model of a pair had the same nose-drag coefficient but different nose shapes. Nose-drag coefficient varied from 0.2 to 1.2. It was found that, within the range of nose shapes and nose drags investigated, induced pressures are functions of nose drag only and are independent of nose shape for axial stations beyond about 1 body diameter downstream of the nose-cylinder junction.

Two blast-wave theories identified as "modified" and "correlated" theories, adequately predicted the induced pressures for nose-drag coefficients above about 0.6 and 0.8, respectively. The adequacy of these theories decreased with decreasing nose drag. Despite the inadequacy of the blast-wave theory to predict these induced pressures in the low-nose-drag range, the parameters developed in the theory in which Mach number was assumed constant correlated the data very well at stations beyond 2.5 body diameters from the nose-cylinder junction, for all the nose drags investigated. The blast-wave parameter in which effect of Mach number was included correlated all the data fairly well, the data being subject to a slight Mach number effect beyond that predicted by blast-wave theory. The only requirement for correlation of the data by the blast-wave parameter was that $M_\infty \sin \sigma$ (M_∞ is free-stream Mach number; σ is semivertex angle of nose) be greater than some limiting value, which for the present investigation was shown to be probably less than 5.

INTRODUCTION

Since the introduction of the concept of blast-wave theory as applied to aerodynamics (refs. 1 to 3), considerable effort has been expended in evaluating its adequacy for the prediction of induced pressures behind blunt noses. (See, for instance, refs. 4 to 12.)

The assumptions upon which blast-wave theory is based are such that its results are apparently applicable over a very limited range in the induced pressure region behind blunt noses. The theory assumes a strong shock in the vicinity of the body. However, since it is also assumed that the square of the tangent of the shock angle is approximately equal to the square of the sine of the shock angle (see ref. 7), the shock cannot be too strong. Thus, the results of the theory are invalid near the nose of the blunt body, where the shock is very strong, and far downstream, where the shock strength deteriorates. Also, because of the assumption of a strong shock, blast-wave theory would not be expected to apply anywhere on bodies with low nose-drag coefficients. Nonetheless it is shown in references 4, 5, and 7 that at hypersonic Mach numbers and zero angle of attack, the blast-wave parameter correlates the theoretical inviscid induced pressures on high-nose-drag, two-dimensional flat plates everywhere except very close to the nose. The theoretical pressures were obtained by the method of characteristics with the leading edge assumed to be a sonic wedge; the nose-drag coefficients were on the order of 1.3 to 1.4.

L 1 5 2 9

In reference 10 the axisymmetric method of characteristics was employed to calculate the theoretical inviscid induced pressures on cylindrical rods with various nose shapes at hypersonic speeds. In the case of reference 10 the nose-drag coefficients varied from about 0.04 to 1.37. The blast-wave parameter correlated the pressure distributions to within a few body diameters of the nose-cylinder junction for all but the lowest nose-drag coefficient investigated.

In reference 8 the induced pressures on cylindrical, flow-alined rods with six different nose shapes were obtained experimentally at a Mach number of 21. The nose-drag coefficients varied from 0.32 to 1.76. The blast-wave theory was inadequate for predicting the induced pressures except in very limited regions as would be expected; however, the blast-wave parameter correlated the induced-pressure data very well along the cylindrical afterbody except close to the nose for all the nose-drag coefficients investigated.

The aforementioned investigations have indicated that the blast-wave theory furnishes a good correlating parameter the usefulness of which extends over a much wider range of nose drags than the assumptions upon which this theory is based would appear to warrant. Also, inherent

in the nose-drag dependence is the implication that induced pressures are independent of nose shape.

In the present paper, the range of validity of the nose-shape-independence concept is investigated experimentally in a systematic manner for the axisymmetric case. Preliminary results of this investigation were included in references 9 and 12. Six pairs of pressure-distribution models were tested. Both models of each pair had the same nose-drag coefficients but different nose shapes. The nose-drag coefficients were 0.2, 0.4, 0.6, 0.8, 1.0, and 1.2. Tests were conducted at nominal free-stream Mach numbers at the model nose of 17.24 and 21.09 with Reynolds numbers based on body diameter and free-stream conditions at the nose of 1.2×10^5 and 0.87×10^5, respectively.

The correlation of the induced pressure is investigated by use of a blast-wave parameter based only on the nose-drag coefficient (Mach number constant) as well as by a blast-wave parameter which includes both nose drag and Mach number effects.

SYMBOLS

A	surface area of model nose, sq in.
C_D	drag coefficient
$C_{D,n}$	nose-drag coefficient
C_p	pressure coefficient
$C_{p,c}$	cone pressure coefficient
$C_{p,max}$	maximum nose pressure coefficient
d	diameter of nose sphere segment, in.
D	maximum cross-sectional diameter of body, in.
l	axial length of nose section, in.
M_∞	free-stream Mach number
p	corrected static pressure, lb/sq in. abs (see eq. (8))
p_m	measured static pressure, lb/sq in. abs

p_s	static pressure at point of junction of nose and cylinder, lb/sq in. abs
p_∞	free-stream static pressure, lb/sq in. abs
$p_{\infty,l}$	local free-stream static pressure, lb/sq in. abs
$p_{\infty,n}$	free-stream static pressure at the apex of the nose, lb/sq in. abs
x,y	Cartesian coordinates (x is distance along axis of symmetry), in.
x_n	axial distance measured from nose apex, in.
x_s	axial distance measured from junction of nose section and cylindrical afterbody, in.
σ	semivertex angle of nose, deg
θ	angle between model x-axis and local surface of nose
η	ratio of induced pressure at infinity divided by the free-stream pressure

MODELS

Six pairs of models (fig. 1) were used in the investigation. The models were 0.125-inch-diameter cylinders approximately 5 inches long with various nose shapes. Pressures were measured at each of seven longitudinal orifice locations from about 0.2 to 20 body diameters behind the nose-cylinder junction. Both models of each pair were designed to have the same nose-drag coefficient. These coefficients were chosen to be $C_{D,n}$ = 0.2, 0.4, 0.6, 0.8, 1.0, and 1.2. One model of each pair had a conical nose, the drag coefficients of which were determined directly from cone calculations (ref. 13) since

$$C_{D,n} = C_{p,c} \tag{1}$$

A plot of $C_{p,c}$ as a function of the semivertex cone angle σ is shown in figure 2. This curve is applicable for both M_∞ = 17 and 21, inasmuch as the difference between pressure coefficients at the two Mach

numbers for any of the cone angles used in this investigation never exceeded 0.5 percent.

The second model of each pair was contoured and its shape was determined from the equation

$$C_{D,n} = \frac{4}{\pi D^2} \int_A C_p \sin \theta dA \tag{2}$$

for each of the specified values of $C_{D,n}$. The configurations for the three highest drag coefficients had noses which were portions of spheres and for these cases the pressure-coefficient distribution was obtained from modified Newtonian theory (ref. 14). The other three configurations had pointed noses and the pressure-coefficient distributions on them were determined from the generalized Newtonian theory of reference 15. It is recognized that Newtonian theory is generally inadequate in the region of the nose-cylinder junction at hypersonic Mach numbers. However, this should have little effect on the integrated nose drag, since the greatest deficiency of the theory occurs in the region of small to zero slope.

The shapes chosen for the contoured noses with $C_{D,n} = 1.2$ and 1.0 were spherical segments, for which case

$$C_{D,n} = \frac{C_{p,max}}{2}\left[2 - \left(\frac{D}{d}\right)^2\right] \tag{3}$$

with $C_{p,max} = 1.76$, and $\frac{d}{D} = 1.254$ and 1.076 for $C_{D,n} = 1.2$ and 1.0, respectively. For $C_{D,n} = 0.8$, a spherically capped cone was chosen for which

$$C_{D,n} = \frac{C_{p,max}}{2}\left[2 \sin^2\theta + \left(\frac{d}{D}\right)^2 \cos^4\theta\right] \tag{4}$$

with $C_{p,max} = 1.76$ and $\theta = 15^\circ$, $\frac{d}{D} = 0.943$. The pointed contoured shapes were taken to be of the form

$$Y = \frac{X}{L}\left(1 - \frac{X}{2}\right) \tag{5}$$

where $Y = \frac{y}{l}$, $X = \frac{x}{l}$, and $L = \frac{l}{D}$. For this case

$$\frac{C_{D,n}}{C_{p,max}} = \left(L^2 + 1\right)\left[2L^2 + 1 - 2L^2\left(L^2 + 1\right)\log_e\left(\frac{L^2 + 1}{L^2}\right)\right] \tag{6}$$

This equation was solved graphically for the variation of $C_{D,n}$ with L. Figure 3 is a plot of $\frac{C_{D,n}}{C_{p,max}}$ against L as given by equation (6). The variation of the semivertex angle σ with L was found from

$$\sigma = \tan^{-1}\left(\frac{dY}{dX}\right)_{X=0} = \tan^{-1}\frac{1}{L} \tag{7}$$

and is shown in figure 4. The variation of $C_{p,max}$ with L is determined from figures 2 and 4. Substituting various combinations of $C_{p,max}$ and L into equation (6) gives the variation of $C_{D,n}$ with L shown in figure 5. The geometric nose shape was found by substituting the value of L for the desired $C_{D,n}$ into equation (5).

INSTRUMENTATION AND ACCURACY

Supply pressures were measured on a bourdon gage with an accuracy of ±0.5 percent. Static pressures were measured on a U-tube butyl phthalate manometer. The reference pressure on the manometer was maintained at less than 20 microns of mercury. The estimated accuracy of the measured static pressures was ±0.0007 lb/sq in. The estimated accuracy of the tunnel Mach number was about ±1.0 percent.

TESTS

All tests were performed in the Langley 2-inch helium tunnel (ref. 6) with the models alined along the axis of the tunnel at zero

angle of attack and zero yaw. From pitot-pressure calibrations and use of the real-gas correction factors from reference 16, it was determined that the tests were performed with free-stream Mach numbers at the nose of the models of 17.24 and 21.09; corresponding test Reynolds numbers based on maximum body diameter and free-stream conditions at the nose were 1.2×10^5 and 0.87×10^5, respectively. Pressures were obtained at stations from 0.2 diameter to 20 diameters behind the nose-cylinder junction.

The small size of the models permitted pressure measurements at only one orifice station per test. Thus, after the pressure at an orifice was measured, this orifice was closed with solder, the body was faired to its original contour, and a new orifice was drilled. All orifices were 0.020 inch in diameter. The surface static pressures were recorded manually at the steady-state condition which was usually obtained about 90 to 120 seconds after initiation of the test.

The 2-inch helium tunnel utilizes a conical nozzle. In order to correct for conical flow effects, the buoyancy correction method discussed in references 8 and 9 was applied to the induced pressure data. Thus, the data are presented as

$$\frac{p}{p_\infty} = \frac{p_m + \left(p_{\infty,n} - p_{\infty,l}\right)}{p_{\infty,n}} \tag{8}$$

RESULTS AND DISCUSSION

The induced pressure data are presented in figures 6 and 7 for $M_\infty = 17.24$ and 21.09, respectively, with p/p_∞ as a function of x_s/d. It can be seen that for a constant nose drag and Mach number the induced pressures $\left(\text{except at } \frac{x_s}{d} = 0.2 \text{ and in some cases at } \frac{x_s}{d} = 1\right)$ are essentially independent of nose shape, in accordance with the implications of blast-wave theory. Also shown on the plots are two theoretical curves. The correlated blast-wave theory is from reference 10 and is given by

$$\frac{p}{p_\infty} = 0.075 \frac{M_\infty^2 \sqrt{C_{D,n}}}{x_s/d} + 0.55 \tag{9}$$

This equation was obtained by correlating the theoretical induced pressures on rods with various nose shapes and free-stream Mach numbers as obtained by characteristics calculations against the blast-wave parameter, and fitting a curve to the correlated characteristic results.

The modified blast-wave theory is from reference 11 with an additional modification to account for the induced pressure levels far downstream which approach greater than free-stream values. (See ref. 8.) The equation for these curves is

$$\frac{p}{p_\infty} = \frac{p_s/p_\infty}{1 + \frac{x_s}{d}} + \eta\left(1 + \frac{1}{x_s/d}\right)^{-\frac{p_s}{p_\infty}\Big/\eta} \qquad (10)$$

where η is the ratio of the induced pressure at infinity divided by the free-stream pressure. Equation (10) is equivalent to that given in reference 11 when $\eta = 1$. The value of p_s/p_∞ was chosen so that the curve passed through the mean of the experimental values of p/p_∞ at $\frac{x_s}{d} = 2.5$, since (as will be shown subsequently) the data were well correlated by the blast-wave parameter beyond this point. The value of η was determined by trial and error under the condition that the curve be in good agreement with the experimental value of p/p_∞ at $\frac{x}{d} = 20$. (It is shown in ref. 8 that induced pressures are essentially independent of nose shape beyond $\frac{x}{d} = 20$, at least for $M_\infty = 21$.) The values of η were thus determined to be 1.26 for all models at $M_\infty = 17.24$ and 1.85 for all models at $M_\infty = 21.09$. Thus η is a function of Mach number or Reynolds number or both.

An examination of figures 6 and 7 reveals that equation (9) (correlated blast-wave theory) is in fair agreement with experiment for the larger values of $C_{D,n}$, whereas equation (10) (modified blast-wave theory) gives good agreement for the larger values of $C_{D,n}$, and the agreement extends to slightly smaller values of $C_{D,n}$ than equation (9). As expected, equation (10) gives better agreement inasmuch as it takes into account viscous effects by utilizing two empirical points $\left(\frac{x_s}{d} = 2.5 \text{ and } \frac{x_s}{d} = 20\right)$. The adequacy of both equation (9) and equation (10) is seen to deteriorate with decreasing $C_{D,n}$.

Despite the inadequacies of the blast-wave theories (eqs. (9) and (10)) for predicting induced pressures in certain regions, the blast-wave parameter is very useful for correlating data, as may be seen from the results presented in figures 8 and 9.

In figures 8(a) and (b) the pressure data are plotted against $\frac{x_s/d}{\sqrt{C_{D,n}}}$ (the blast-wave parameter for constant M_∞) for $M_\infty = 17.24$ and 21.09, respectively. The induced pressures for all nose drags and shapes are seen to correlate with this parameter for x_s/d greater than 2.5.

Also shown in figures 8(a) and (b) are curves calculated by equations (9) and (10) (refs. 10 and 11, respectively). The calculation by equation (10) is shown for the case where $C_{D,n} = 1.0$, since this nose shape most closely corresponds to the leading edge for which equation (10) was proposed in reference 11.

Figure 9 is a plot of the induced pressure ratio as a function of the blast-wave parameter in which Mach number effects are included. In figure 9(a) the orifice locations are measured from the nose-cylinder junction and in figure 9(b) they are measured from the nose. The form of data presentation in figure 9(b) is used because the theoretical curve (eq. (9)) was obtained in reference 10 by assuming orifice locations measured from the nose. The data in this figure are well correlated by the blast-wave parameter at stations beyond x_s/d of about 2.5. Whether the method of 9(a) or 9(b) is to be preferred appears to be a matter of choice. A comparison of figures 8 and 9 indicates better correlation of the data with nose drag at constant Mach number than with both nose drag and Mach number effects included, the data being subject to a slight Mach number effect beyond that predicted by the blast-wave parameter.

Again, equations (9) and (10) (refs. 10 and 11, respectively) are shown in figures 9(a) and (b). As in the case of figures 8(a) and (b), the calculation by equation (10) (ref. 11) is for the case where $C_{D,n} = 1.0$. As was previously mentioned, the fact that the method of reference 11 gives better agreement with the data is due largely to the use of empirical end points.

Figure 10 shows a comparison of the results of the present investigation with those obtained in reference 8. The slight displacement of the data may possibly be attributed to Reynolds number. Reynolds numbers based on body diameters for the present investigation and that of reference 8 were, for $M_\infty \approx 21$, 0.87×10^5 and 0.62×10^5, respectively.

Since the blast-wave theory required a strong shock, it is, at first glance, surprising that the parameter developed in the theory is useful for correlating the data for a drag coefficient as low as 0.2. However, it has been pointed out in reference 17 that the assumption of a strong shock implies that $M_\infty \sin \sigma \gg 1$. The information contained in reference 13 can be utilized to show that for cones in helium flow

$$M_\infty \sin \sigma = \frac{M_\infty \sqrt{C_{D,n}}}{1.49}$$

From this equation it is seen that the lowest value of $M_\infty \sin \sigma$ attained in these tests was 5.1. Although 5.1 is not an order of magnitude greater than 1, it is apparently sufficient for the correlation of data by the blast-wave parameter. It is probable that the nose-shape-independence concept will hold for values of $M_\infty \sin \sigma$ somewhat less than 5. The lower limit can only be determined by additional experiment.

Thus, although the blast-wave theories of references 10 and 11 (eqs. (9) and (10)) require a high nose-drag coefficient, the parameters developed in the theories will correlate data provided only that $M_\infty \sin \sigma$ be greater than some limiting value, which as shown above is probably less than 5.

CONCLUSIONS

The range of validity of the nose-shape-independence concept of the blast-wave theory has been investigated in a systematic manner by the use of six pairs of pressure models. Induced pressure distributions were obtained at zero angle of attack with free-stream Mach numbers of about 17 and 21. Each model of a pair had the same nose-drag coefficient, but different nose shapes. Nose-drag coefficient varied from 0.2 to 1.2. As a result of these tests, the following conclusions were drawn.

1. Within the range of nose shapes and drags investigated, induced pressures are, in general, functions of nose drag only and appear to be independent of nose shape at stations beyond about 1 body diameter downstream of the nose-cylinder junction.

2. At constant Mach number, the blast-wave parameter correlates the data well for all nose drags at stations beyond 2.5 body diameters from the nose-cylinder junction.

3. The blast-wave parameter that includes Mach number effect is helpful in correlating the data. However, a slight Mach number effect beyond that predicted by blast-wave theory is indicated.

4. Both a modified and a correlated blast-wave theory adequately predict the induced pressures for nose-drag coefficients above about 0.6 and 0.8, respectively. At lower nose-drag coefficients these theories are inadequate.

5. Although the blast-wave theories of Vernon Van Hise (NASA TR R-78) and of E. S. Love (ARS Jour., Oct. 1959) require a high nose-drag coefficient, the parameters developed in the theories appear to correlate data provided only that the product of the Mach number and the sine of the semivertex cone angle be greater than some limiting value, which for the present investigation is indicated to be less than 5.

Langley Research Center,
National Aeronautics and Space Administration,
Langley Air Force Base, Va., March 7, 1962.

REFERENCES

1. Cheng, H. K., and Pallone, A. J.: Inviscid Leading-Edge Effect in Hypersonic Flow. Jour. Aero. Sci. (Readers' Forum), vol. 23, no. 7, July 1956, pp. 700-702.

2. Lin, Shao-Chi: Cylindrical Shock Waves Produced by Instantaneous Energy Release. Jour. Appl. Phys., vol. 25, no. 1, Jan. 1954, pp. 54-57.

3. Lees, Lester, and Kubota, Toshi: Inviscid Hypersonic Flow Over Blunt-Nosed Slender Bodies. Jour. Aero. Sci., vol. 24, no. 3, Mar. 1957, pp. 195-202.

4. Bertram, M. H., and Baradell, D. L.: A Note on the Sonic-Wedge Leading-Edge Approximation in Hypersonic Flow. Jour. Aero. Sci. (Readers' Forum), vol. 24, no. 8, Aug. 1957, pp. 627-629.

5. Bertram, Mitchel H., and Henderson, Arthur, Jr.: Effects of Boundary-Layer Displacement and Leading-Edge Bluntness on Pressure Distribution, Skin Friction, and Heat Transfer of Bodies at Hypersonic Speeds. NACA TN 4301, 1958.

6. Henderson, Arthur, Jr., and Johnston, Patrick J.: Fluid-Dynamic Properties of Some Simple Sharp- and Blunt-Nosed Shapes at Mach Numbers From 16 to 24 in Helium Flow. NASA MEMO 5-8-59L, 1959.

7. Baradell, Donald L., and Bertram, Mitchel H.: The Blunt Plate in Hypersonic Flow. NASA TN D-408, 1960.

8. Mueller, James N., Close, William H., and Henderson, Arthur, Jr.: An Investigation of Induced-Pressure Phenomena on Axially Symmetric, Flow-Alined, Cylindrical Models Equipped With Different Nose Shapes at Free-Stream Mach Numbers From 15.6 to 21 in Helium. NASA TN D-373, 1960.

9. Henderson, Arthur, Jr.: Investigation of the Flow Over Simple Bodies at Mach Numbers of the Order of 20. NASA TN D-449, 1960.

10. Van Hise, Vernon: Analytical Study of Induced Pressure on Long Bodies of Revolution With Varying Nose Bluntness at Hypersonic Speeds. NASA TR R-78, 1961.

11. Love, E. S.: Prediction of Inviscid Induced Pressures from Round Leading Edge Blunting at Hypersonic Speeds. ARS Jour. (Tech. Notes), vol. 29, no. 10, pt. 1, Oct. 1959, pp. 792-794.

12. Bertram, Mitchel H., and Henderson, Arthur, Jr.: Recent Hypersonic Studies of Wings and Bodies. ARS Jour., vol. 31, no. 8, Aug. 1961, pp. 1129-1139.

13. Henderson, Arthur, Jr., and Braswell, Dorothy O.: Charts for Conical and Two-Dimensional Oblique-Shock Flow Parameters in Helium at Mach Numbers From About 1 to 100. NASA TN D-819, 1961.

14. Lees, Lester: Hypersonic Flow. Fifth International Aeronautical Conference (Los Angeles, Calif., June 20-23, 1955), Inst. Aero. Sci., Inc., 1955, pp. 241-276.

15. Love, E. S.: Generalized Newtonian Theory. Jour. Aero/Space Sci., (Readers' Forum), vol. 26, no. 5, May 1959, pp. 314-315.

16. Erickson, Wayne D.: Real-Gas Correction Factors for Hypersonic Flow Parameters in Helium. NASA TN D-462, 1960.

17. Hayes, Wallace D., and Probestein, Ronald F.: Hypersonic Flow Theory. Academic Press, Inc. (New York), 1959.

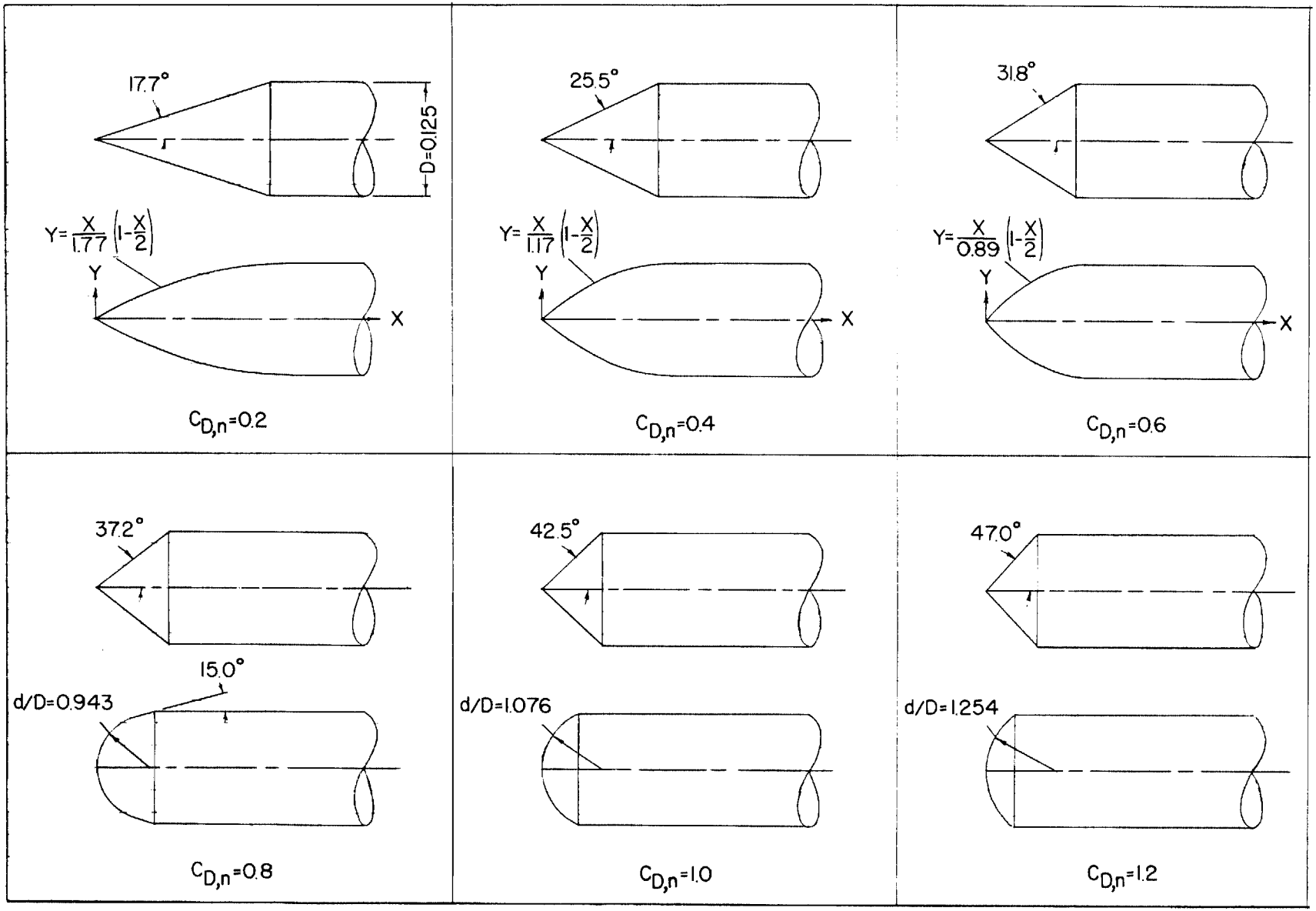

Figure 1.- Nose shapes of investigation.

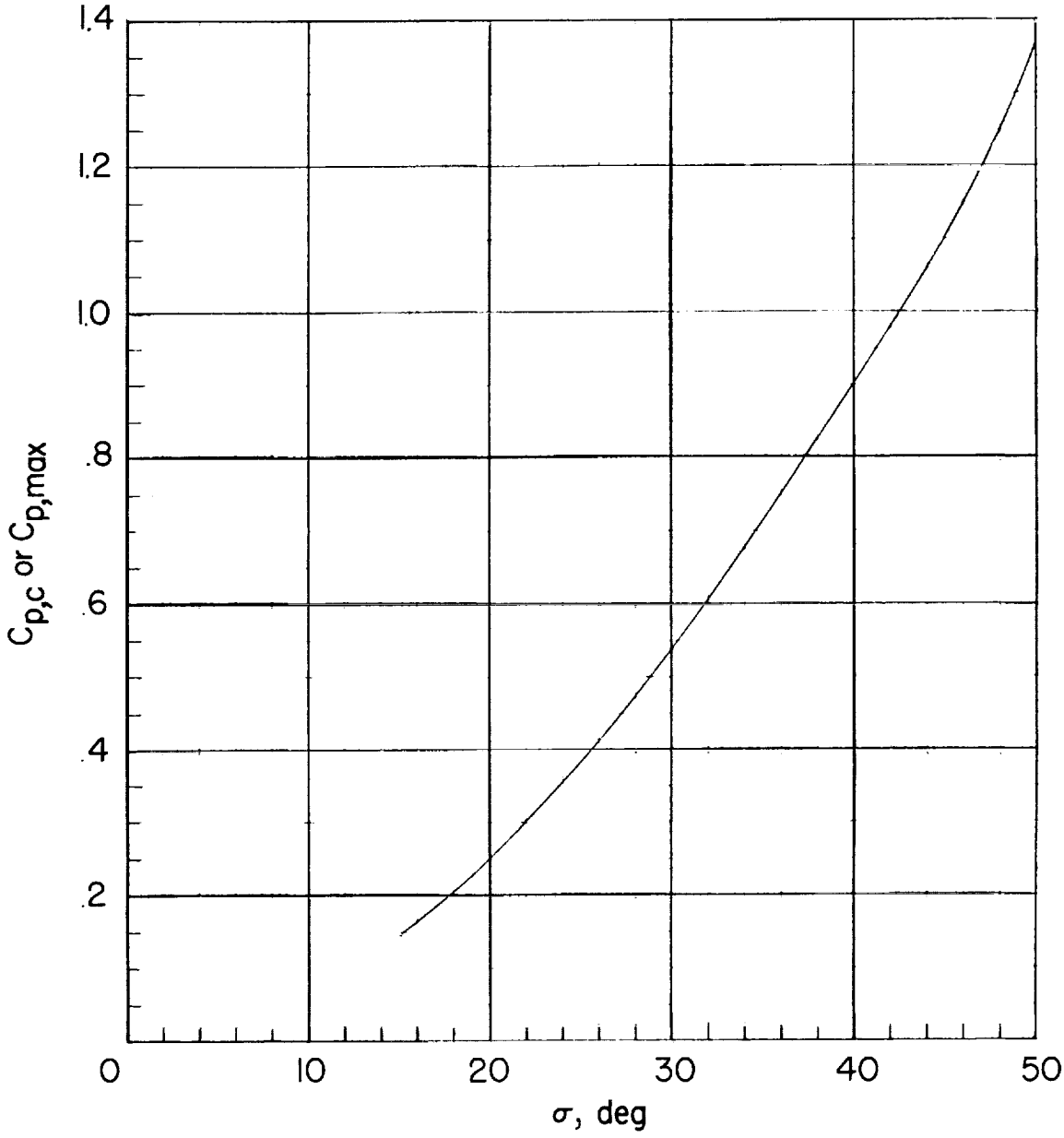

Figure 2.- Variation of cone pressure coefficient with cone semiangle.

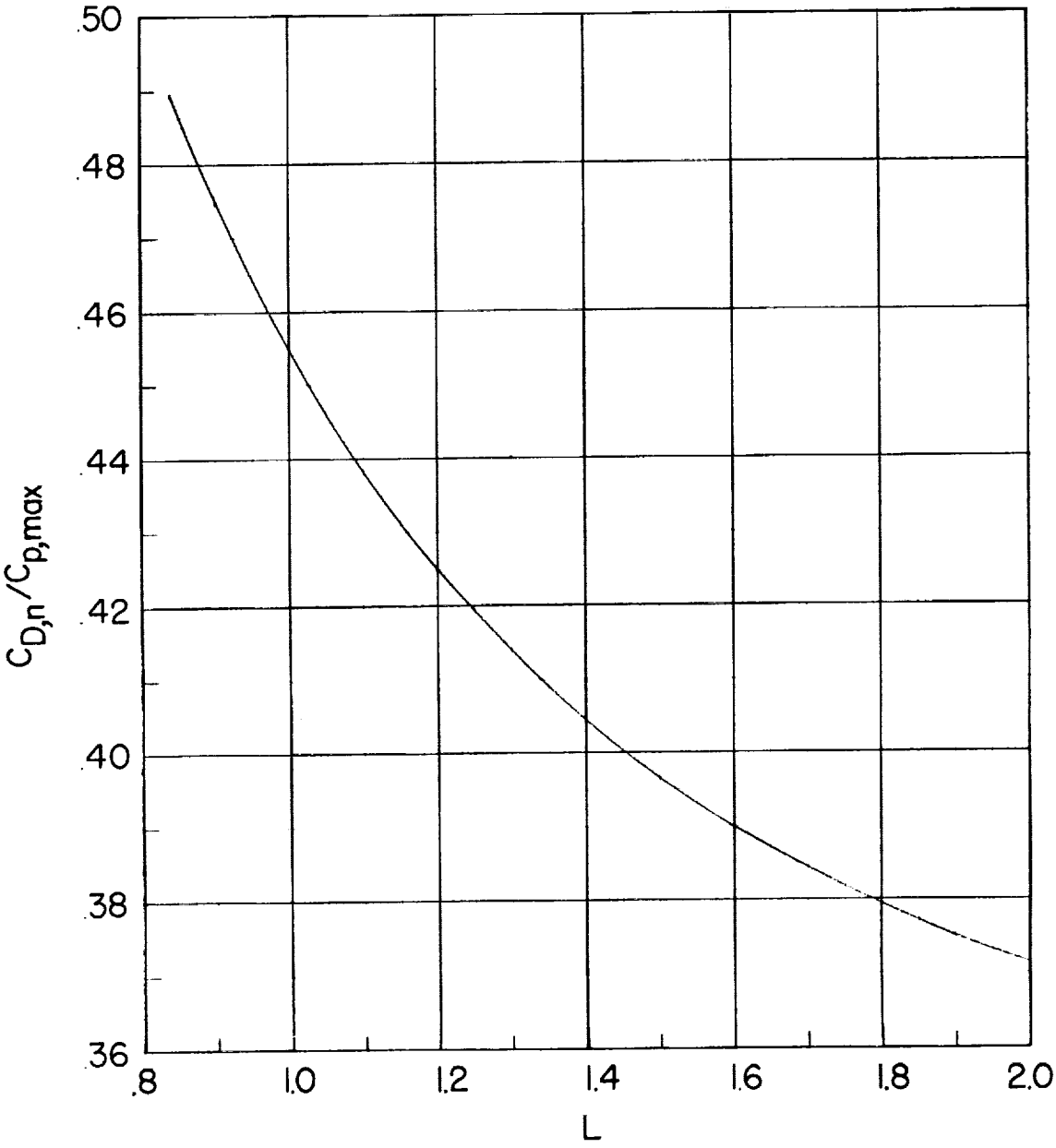

Figure 3.- Variation of ratio of nose-drag coefficient to maximum pressure coefficient on sharp-nose bodies with length-diameter ratio L (from eq. (6)).

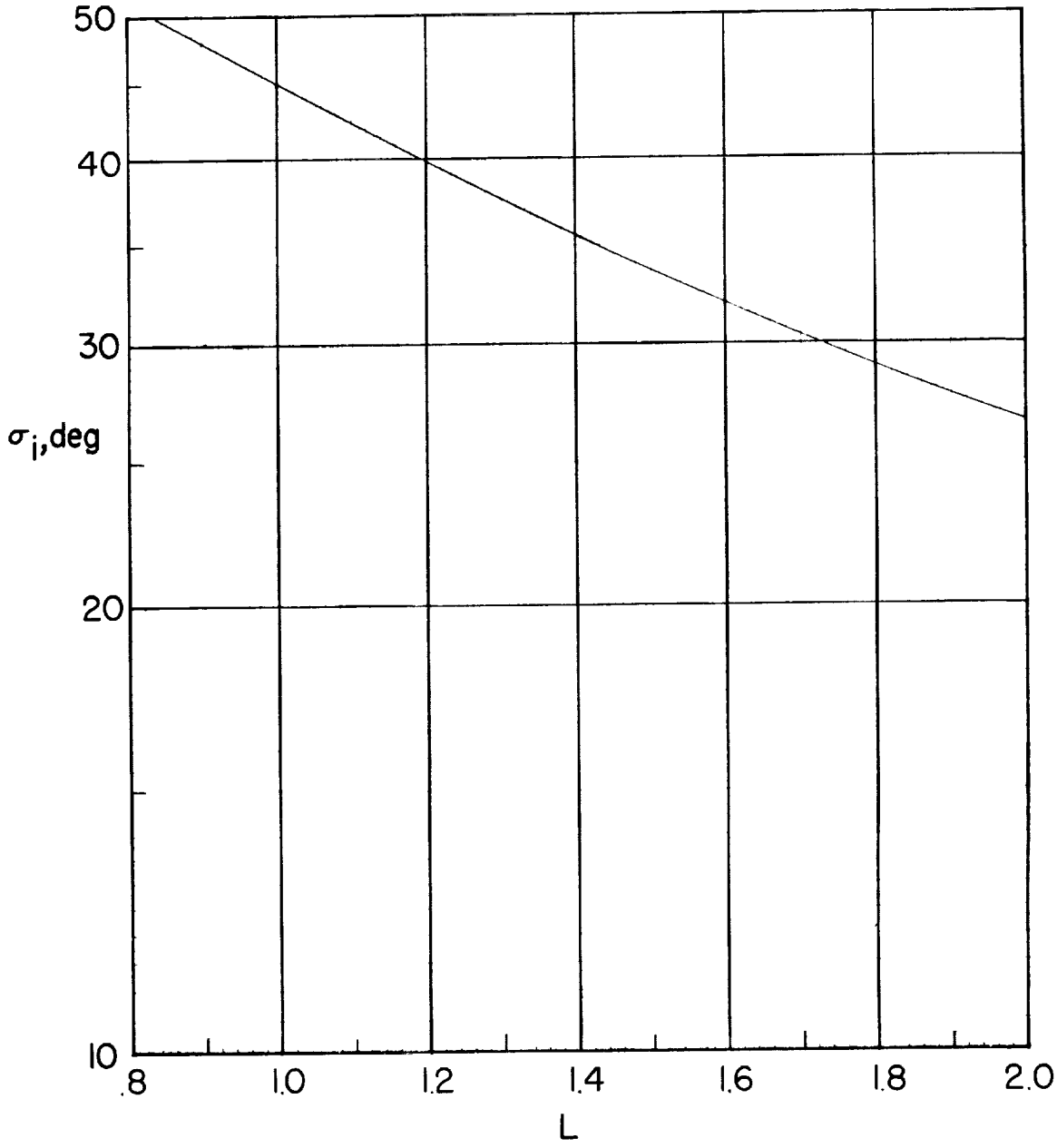

Figure 4.- Variation of cone semivertex angle on sharp-nose body with length-diameter ratio L (from eq. (7)).

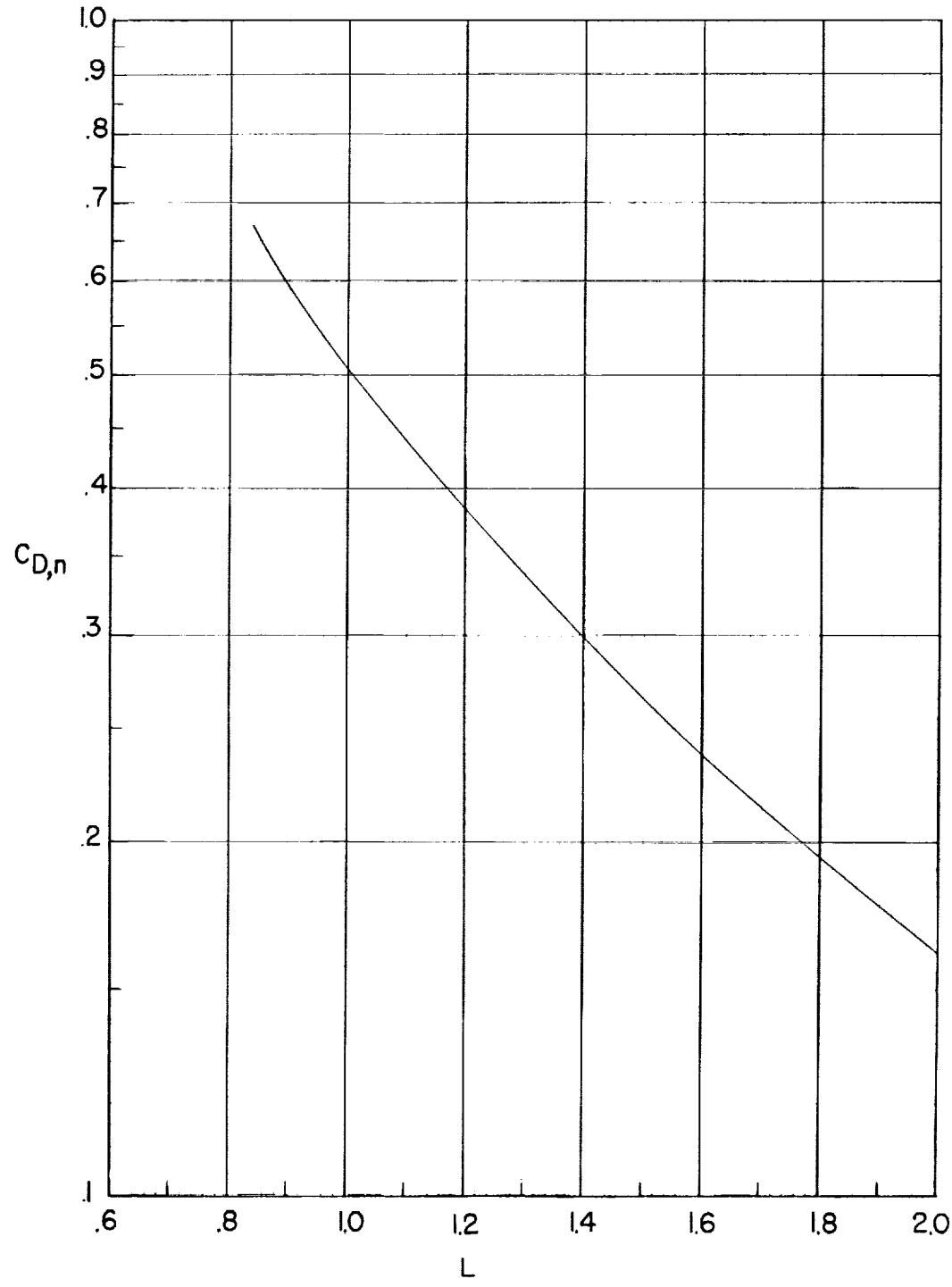

Figure 5.- Variation of nose-drag coefficients with length-diameter ratio L for sharp-nose bodies.

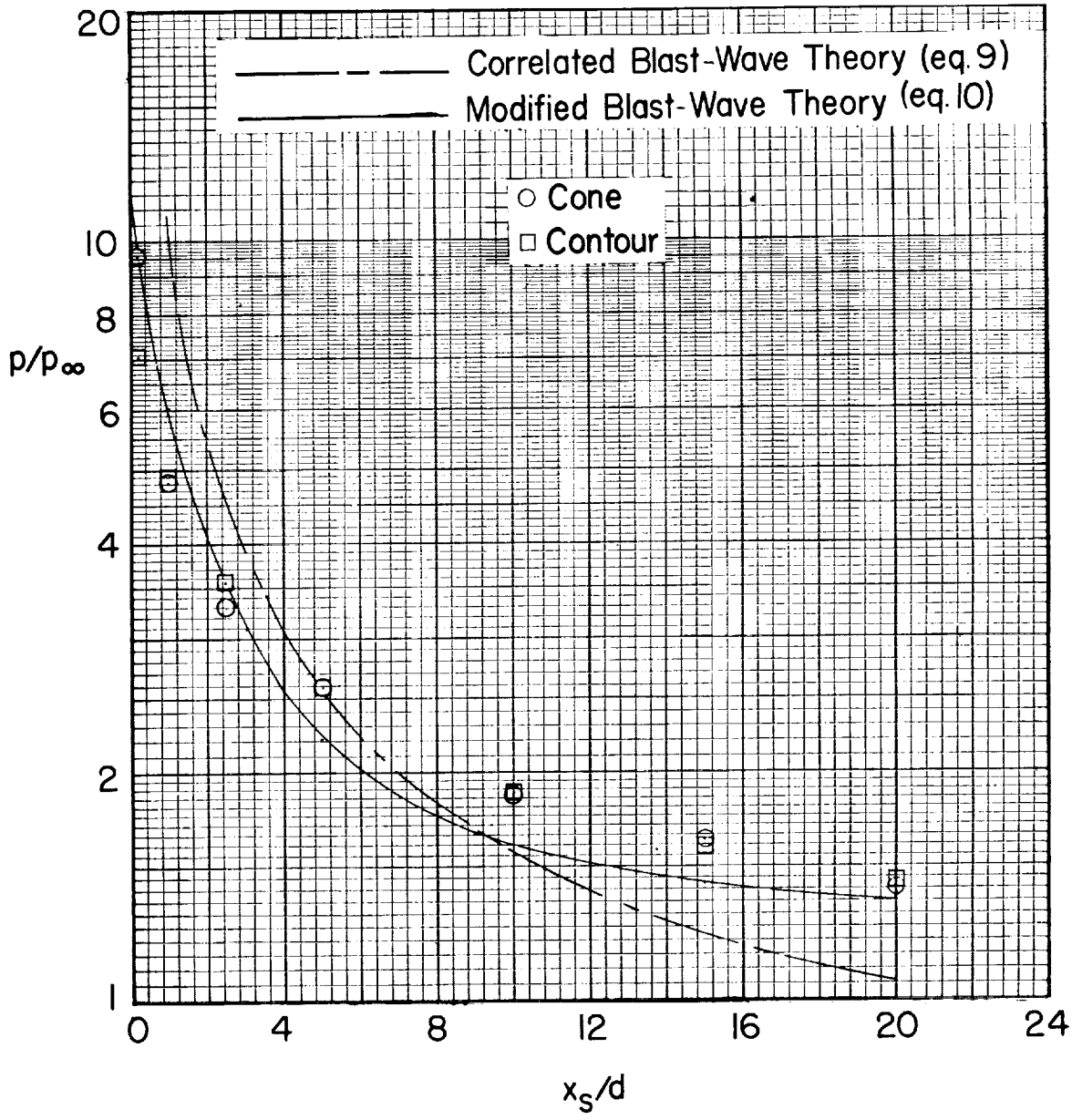

(a) $C_{D,n} = 0.2$.

Figure 6.- Variation of induced pressure with distance from nose-cylinder juncture at $M_\infty = 17.24$.

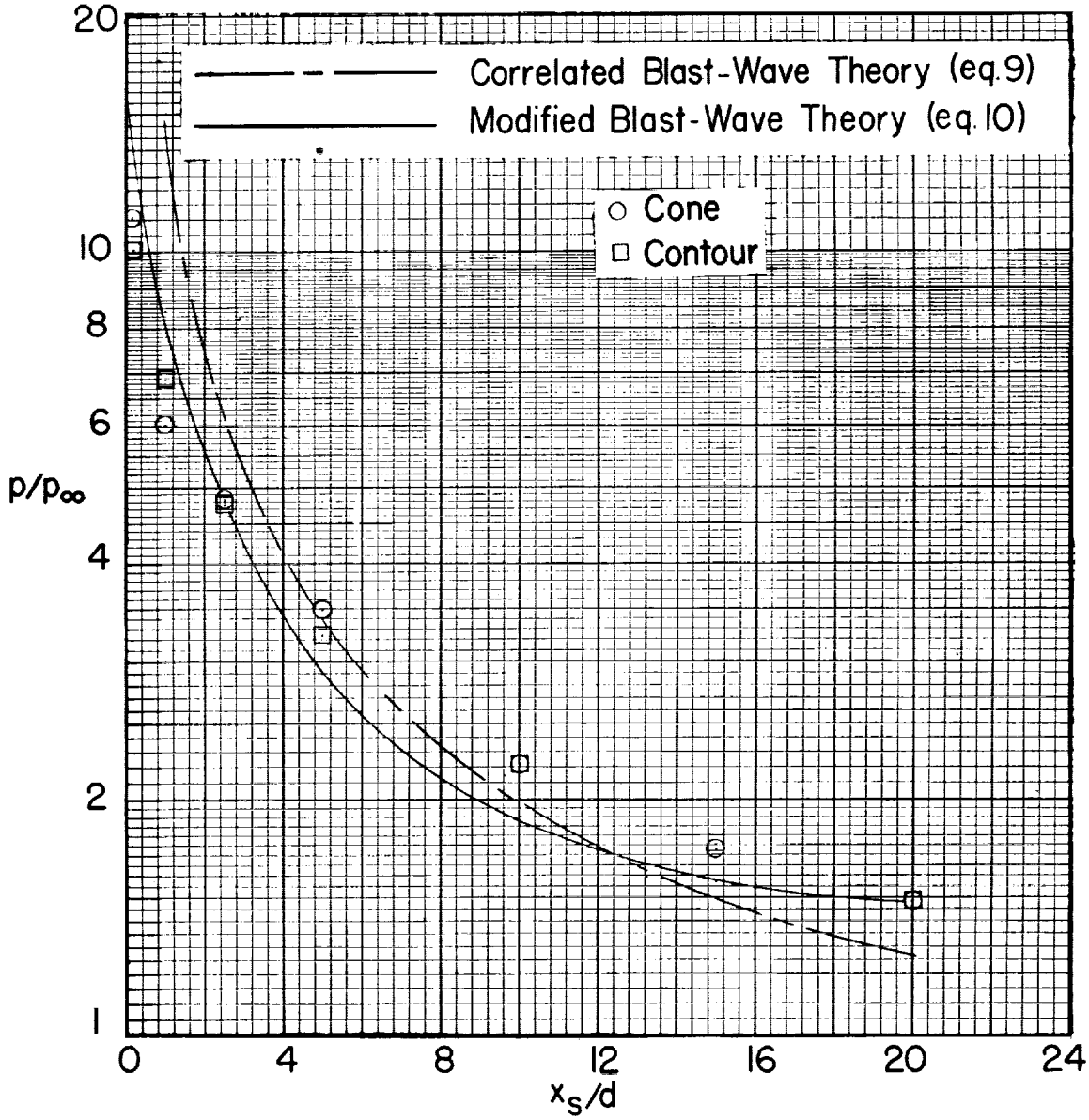

(b) $C_{D,n} = 0.4$.

Figure 6.- Continued.

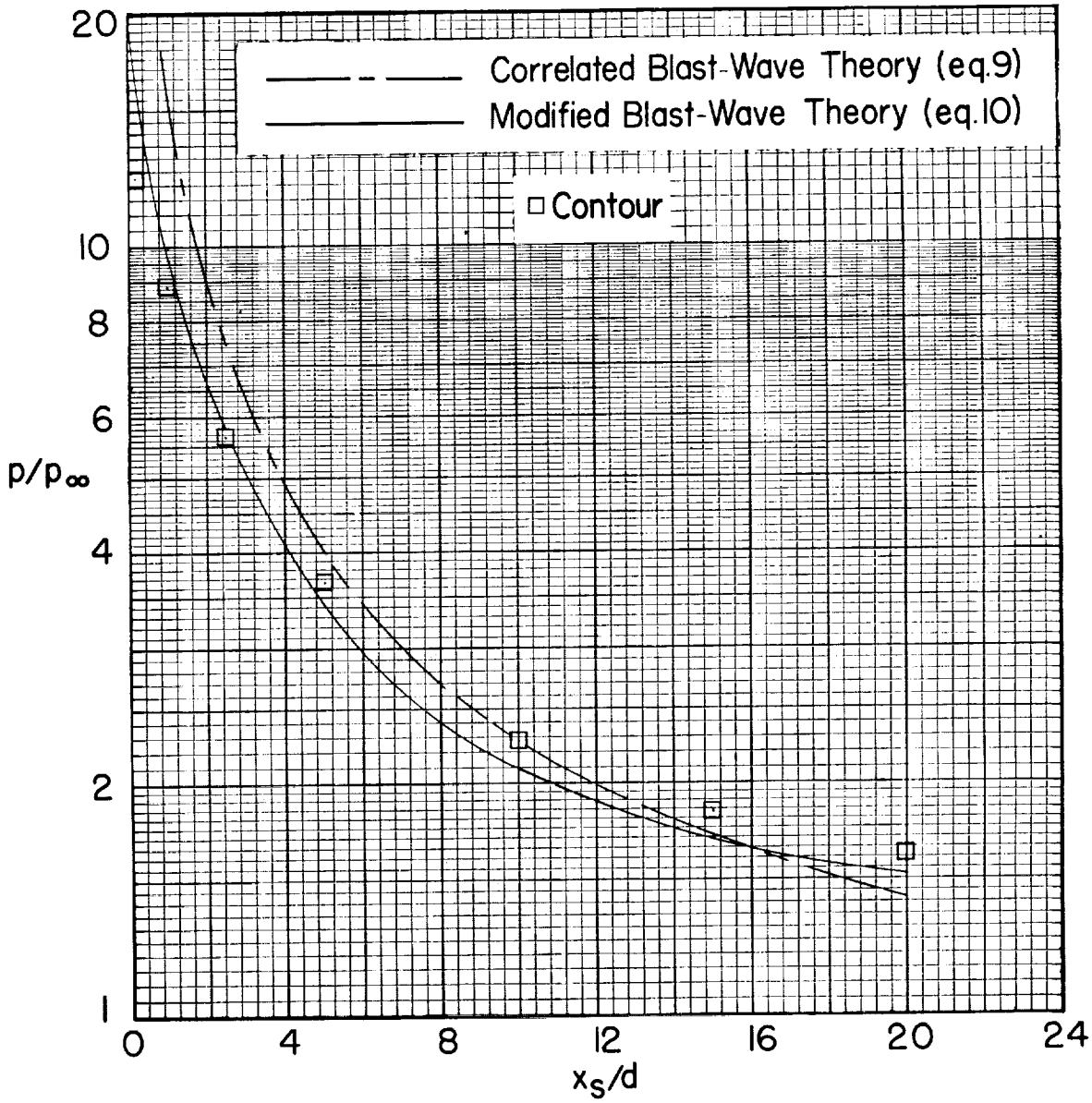

(c) $C_{D,n} = 0.6$.

Figure 6.- Continued.

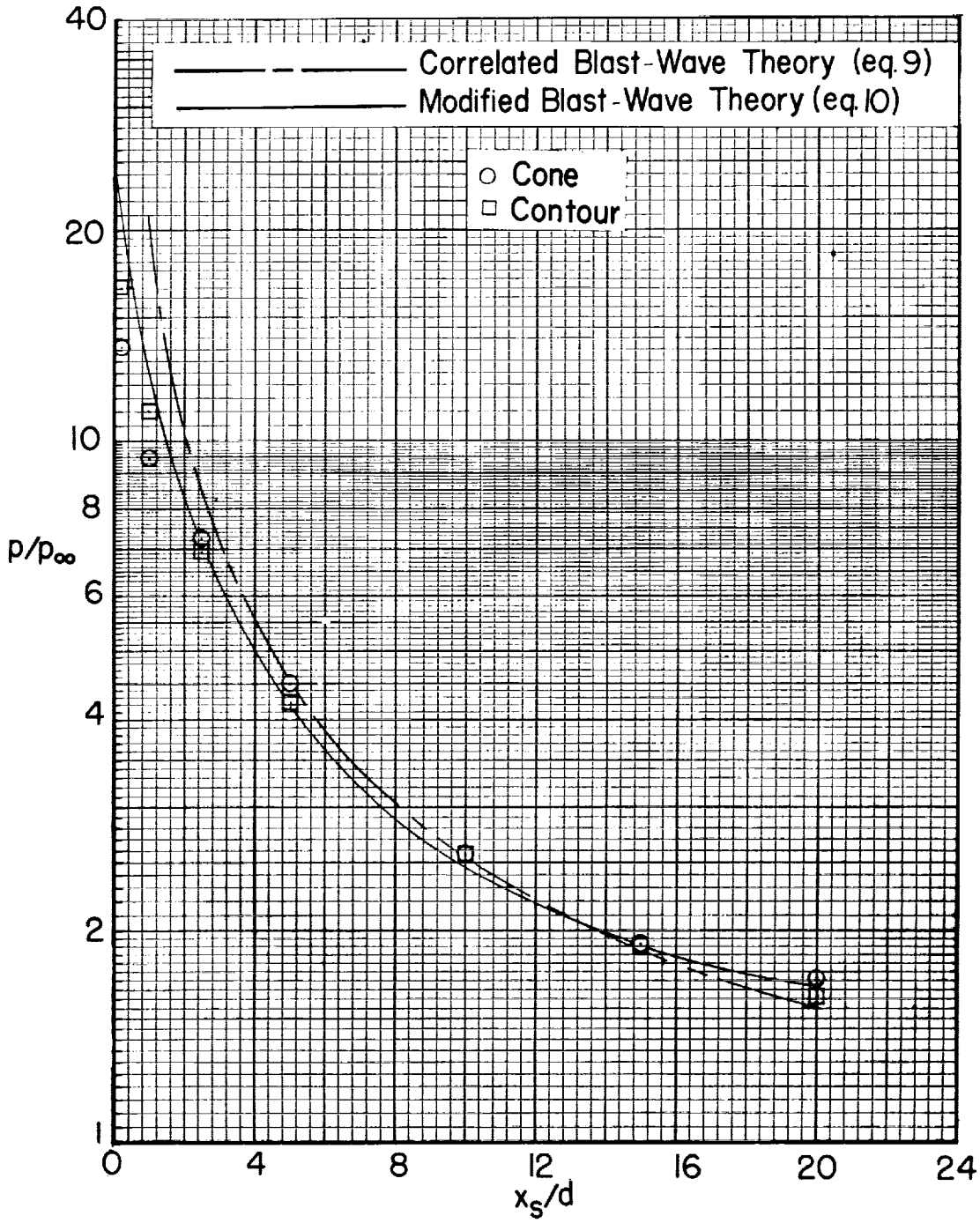

(d) $C_{D,n} = 0.8$.

Figure 6.- Continued.

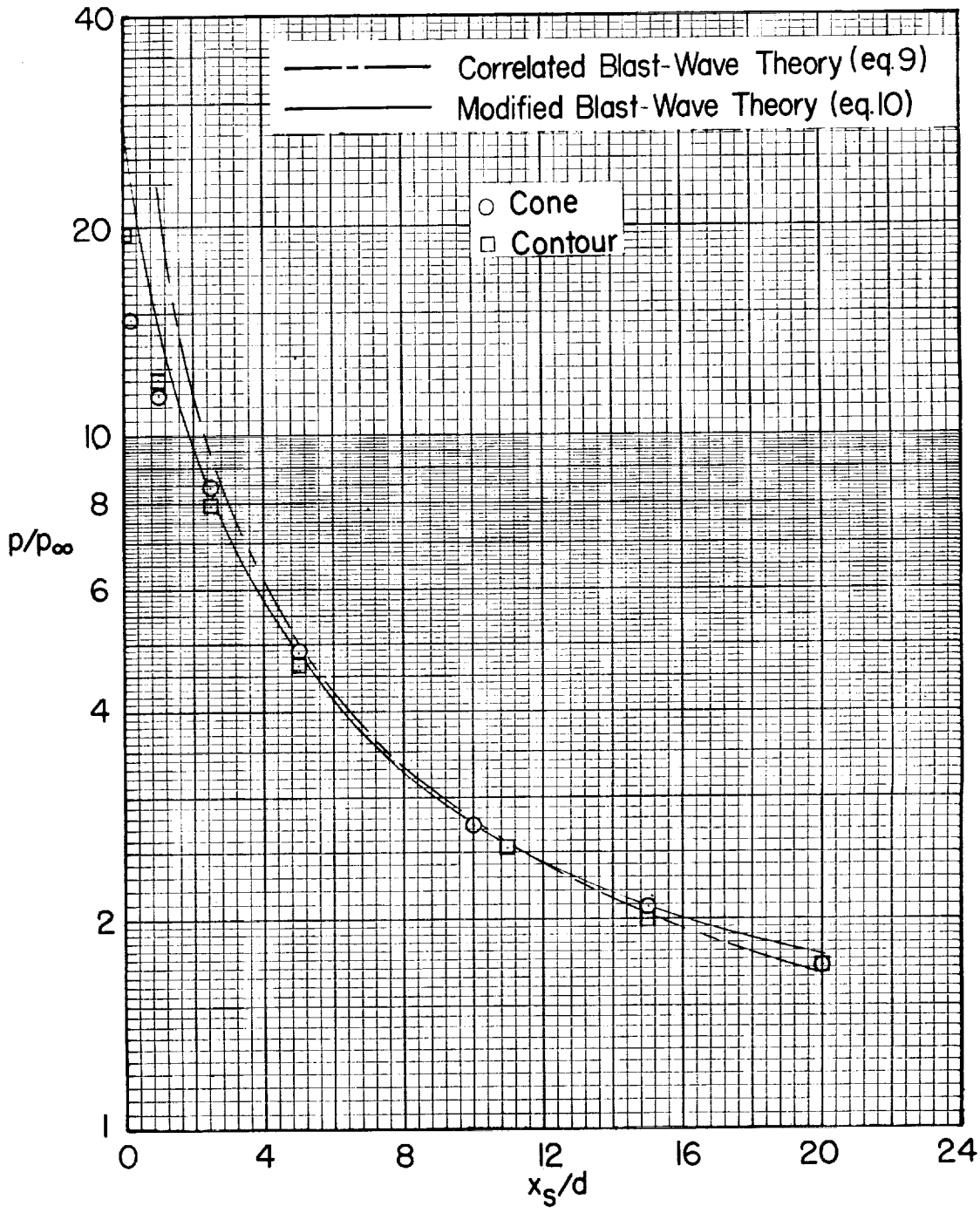

(e) $C_{D,n} = 1.0$.

Figure 6.- Continued.

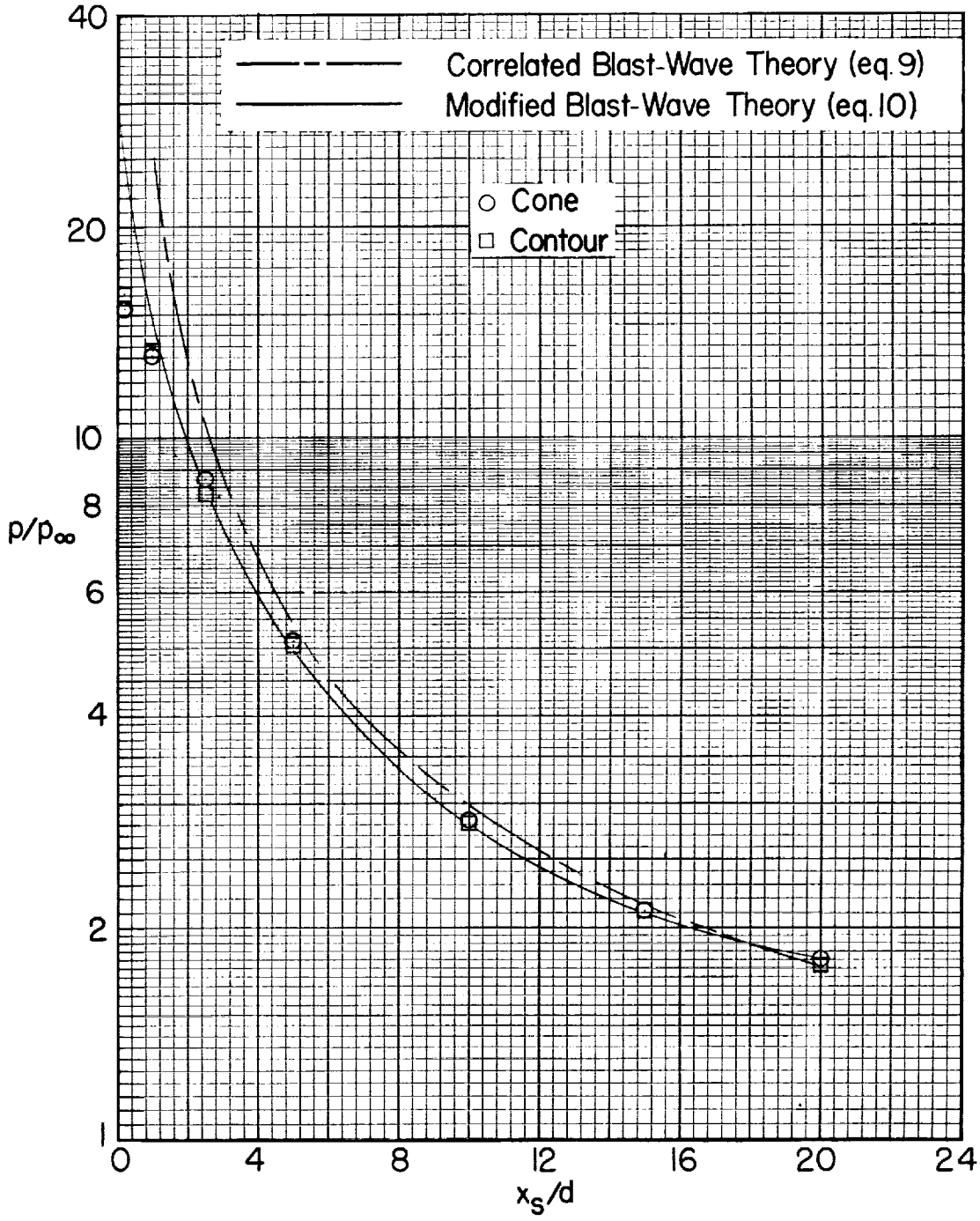

(f) $C_{D,n} = 1.2$.

Figure 6.- Concluded.

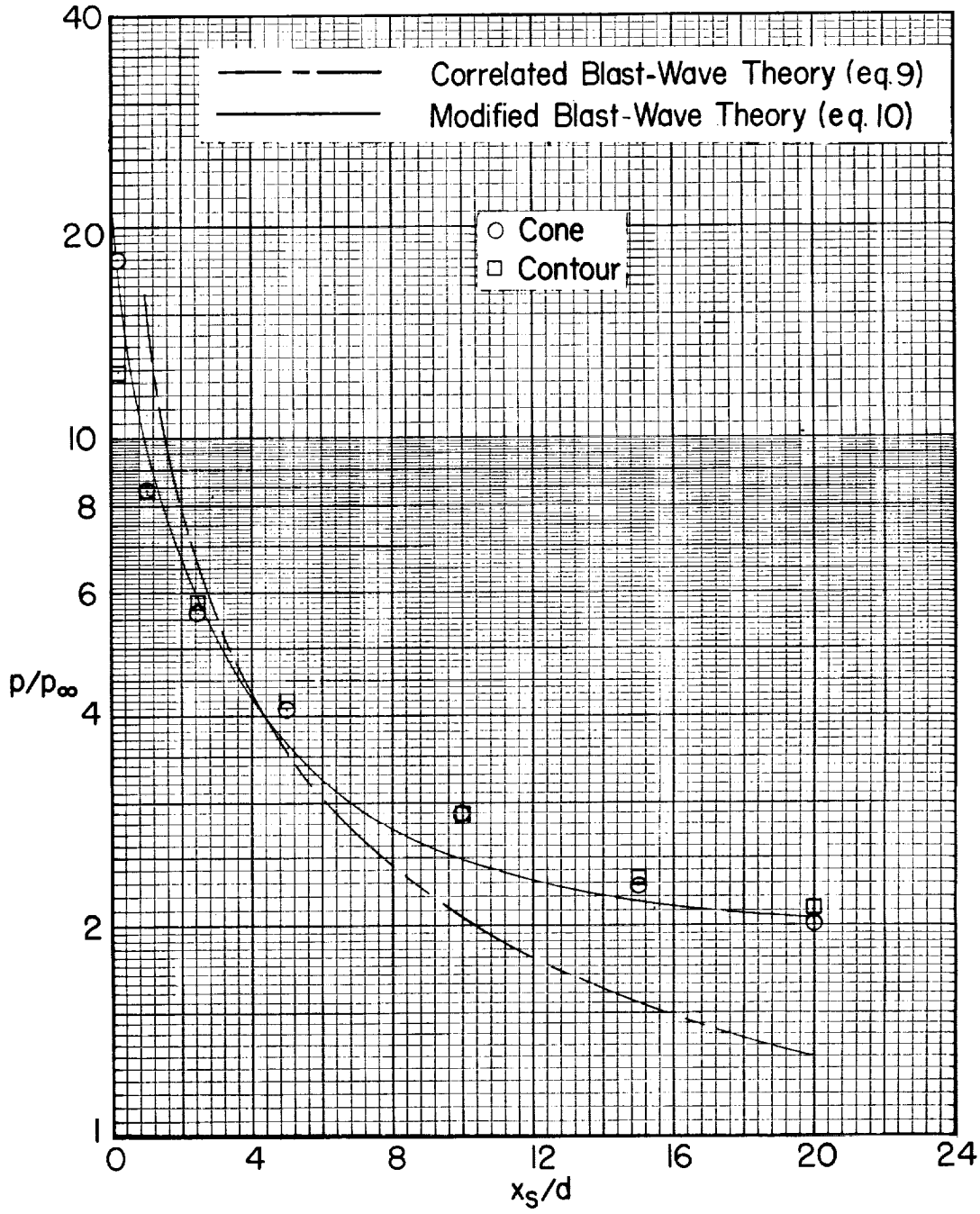

(a) $C_{D,n} = 0.2$.

Figure 7.- Variation of induced pressure with distance from nose-cylinder juncture at $M_\infty = 21.09$.

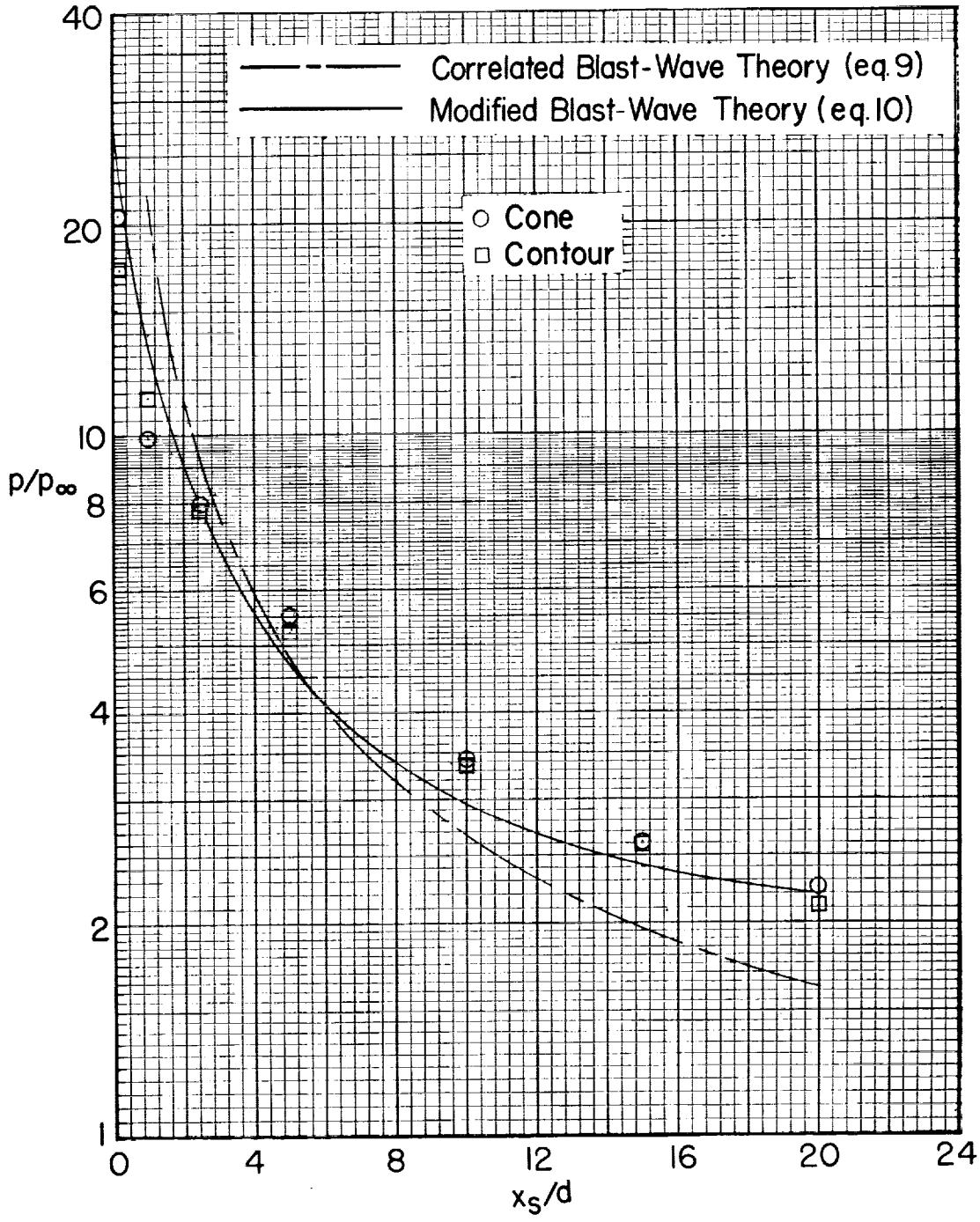

(b) $C_{D,n} = 0.4$.

Figure 7.- Continued.

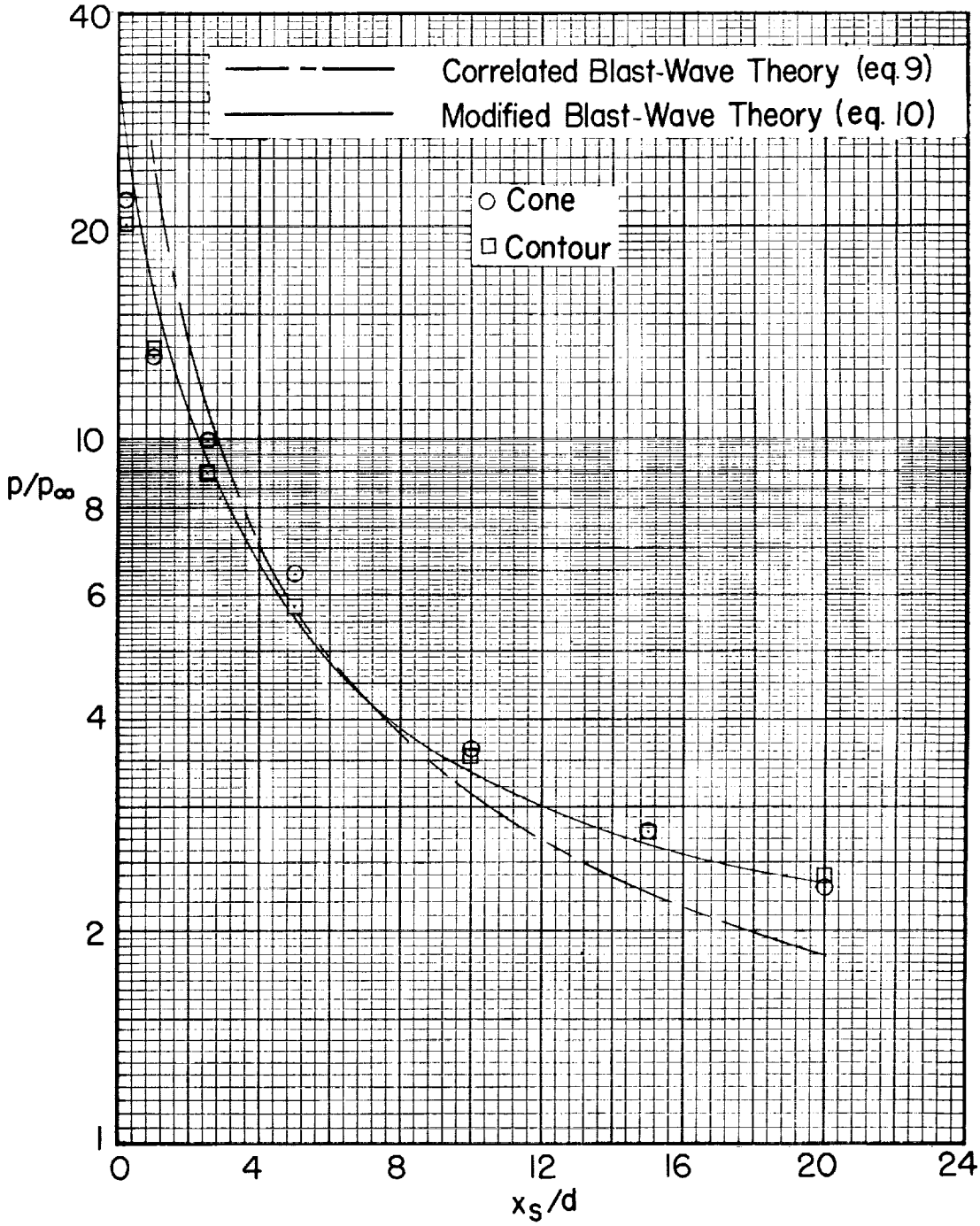

(c) $C_{D,n} = 0.6$.

Figure 7.- Continued.

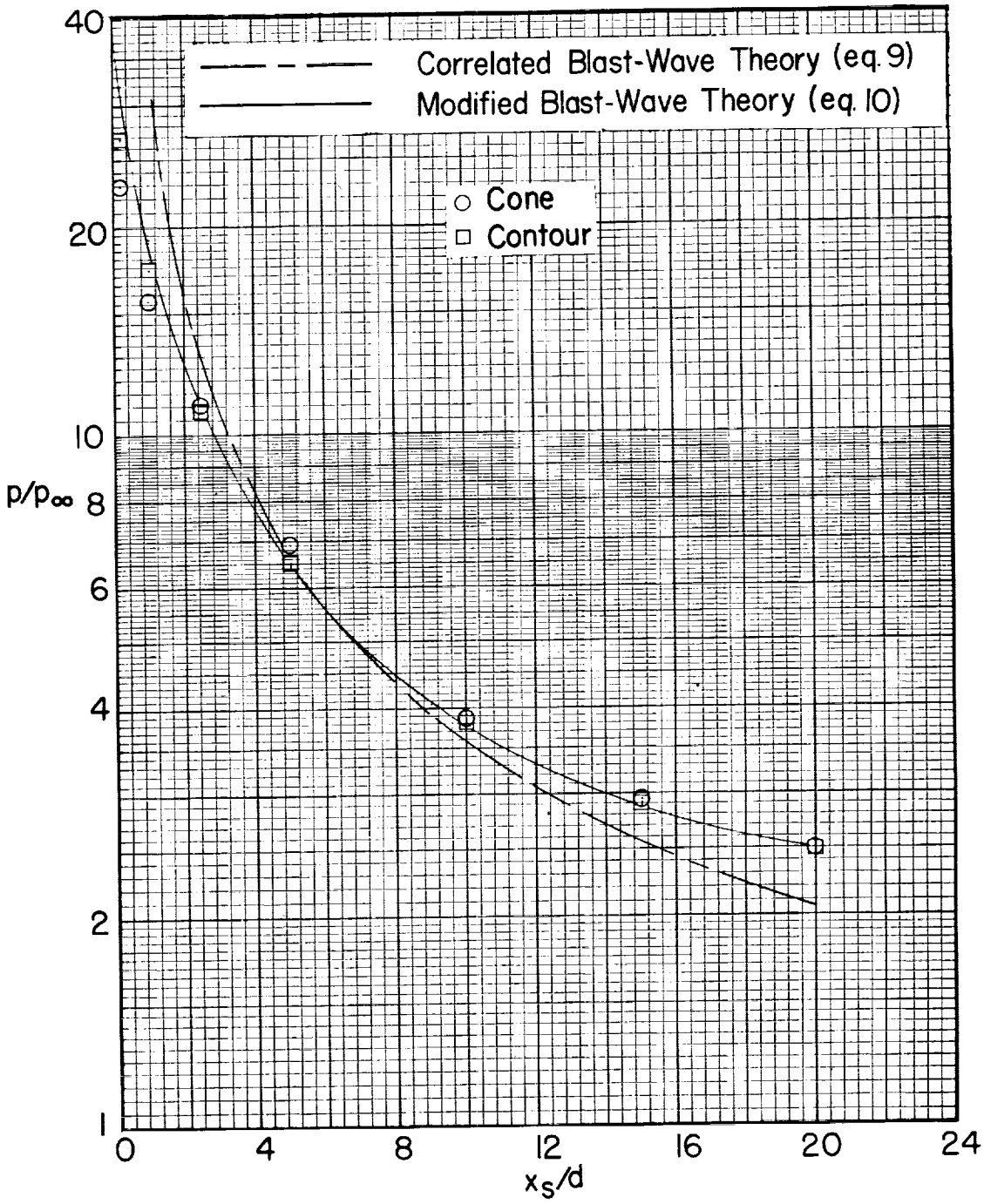

(d) $C_{D,n} = 0.8$.

Figure 7.- Continued.

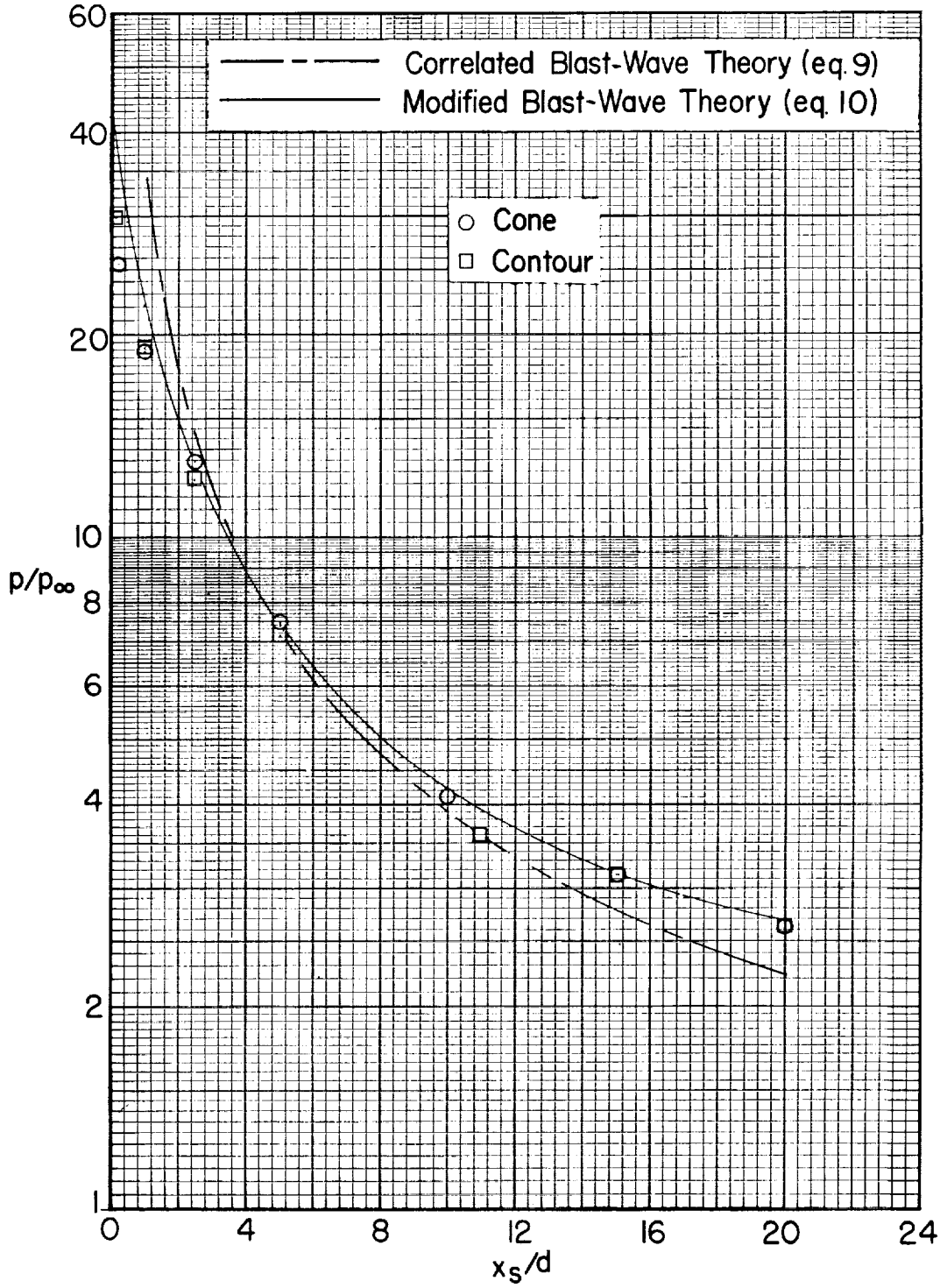

(e) $C_{D,n} = 1.0$.

Figure 7.- Continued.

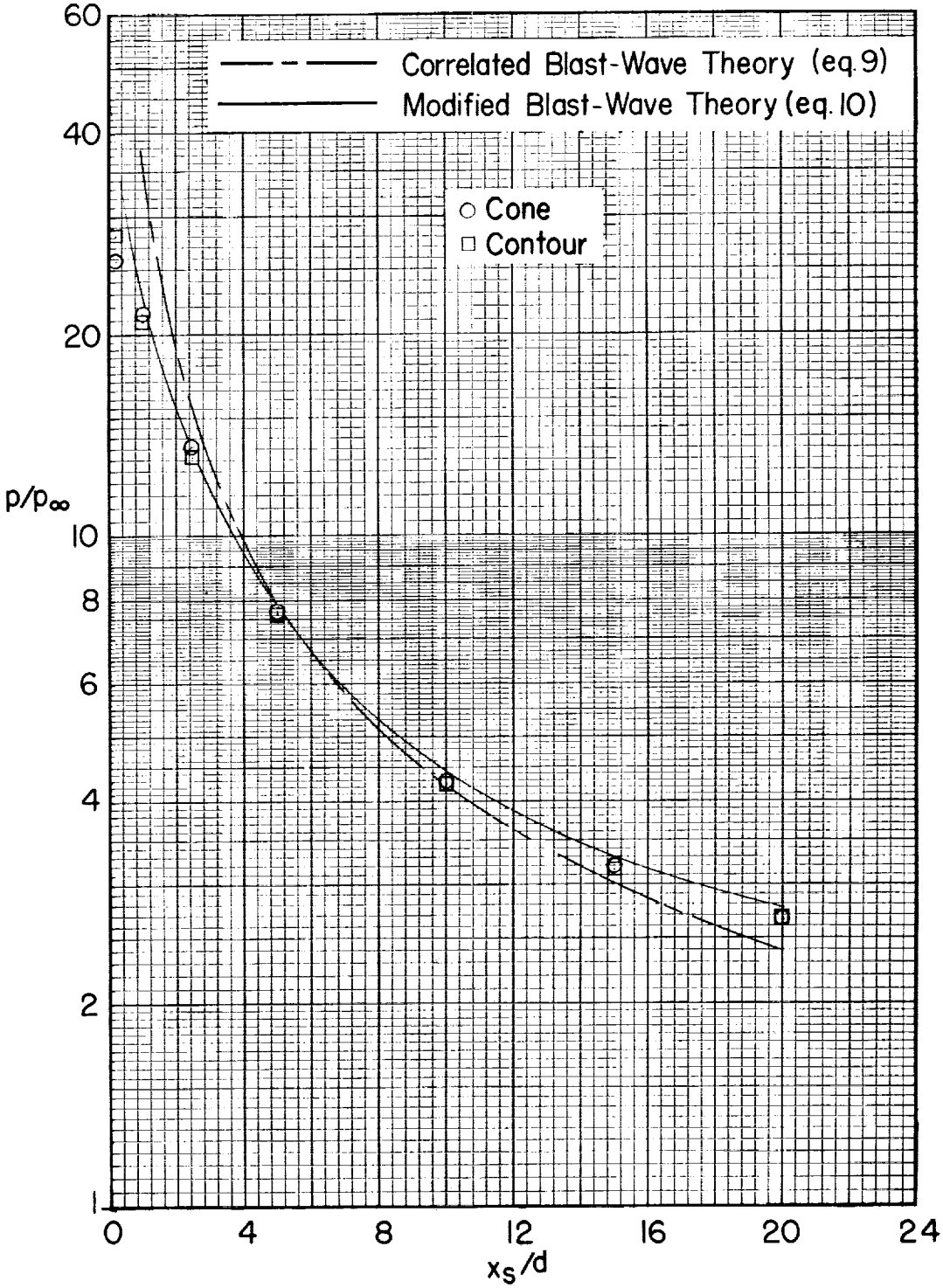

(f) $C_{D,n} = 1.2$.

Figure 7.- Concluded.

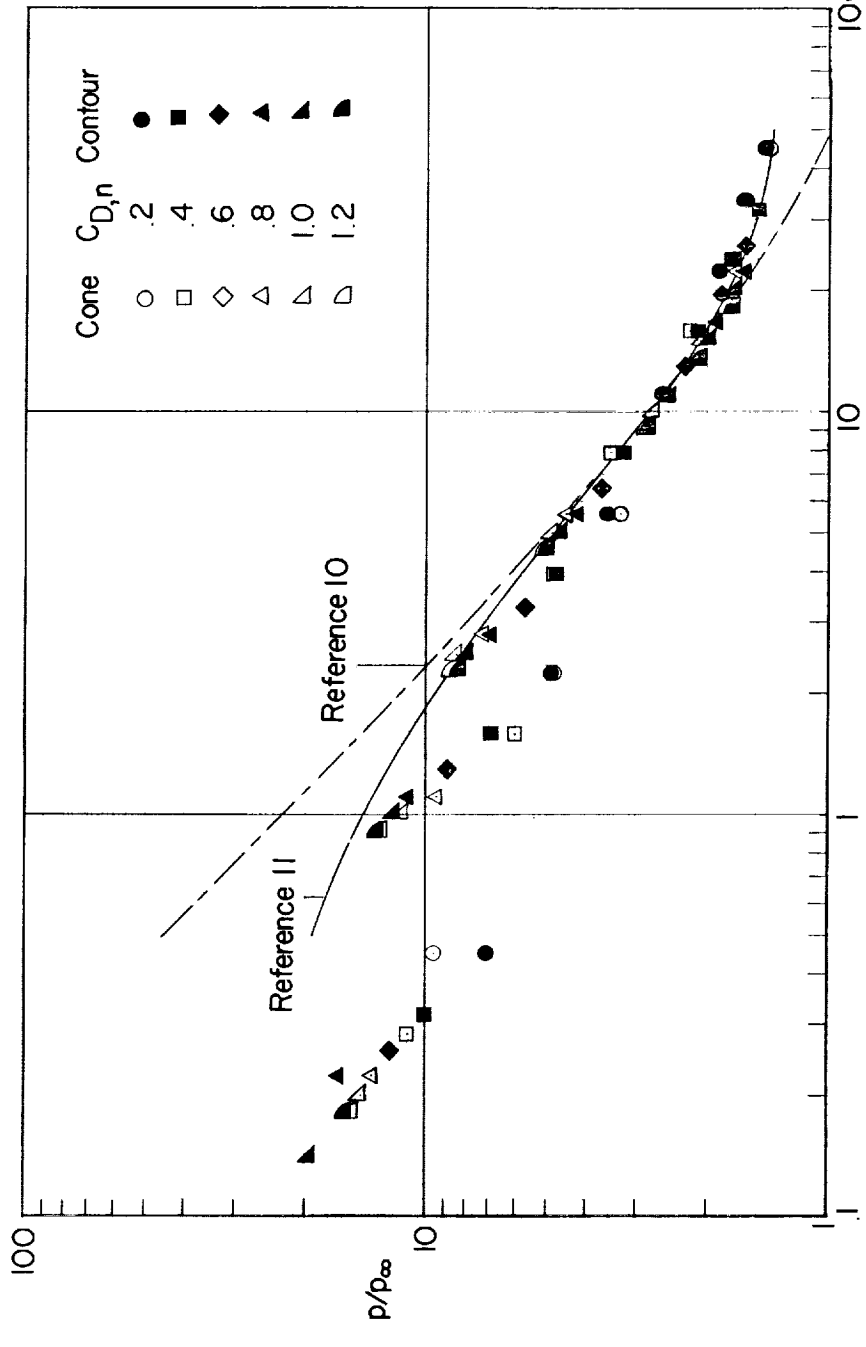

(a) $M_\infty = 17.24$.

Figure 8.- Correlation of induced pressures with blast-wave parameter based only on nose-drag coefficient.

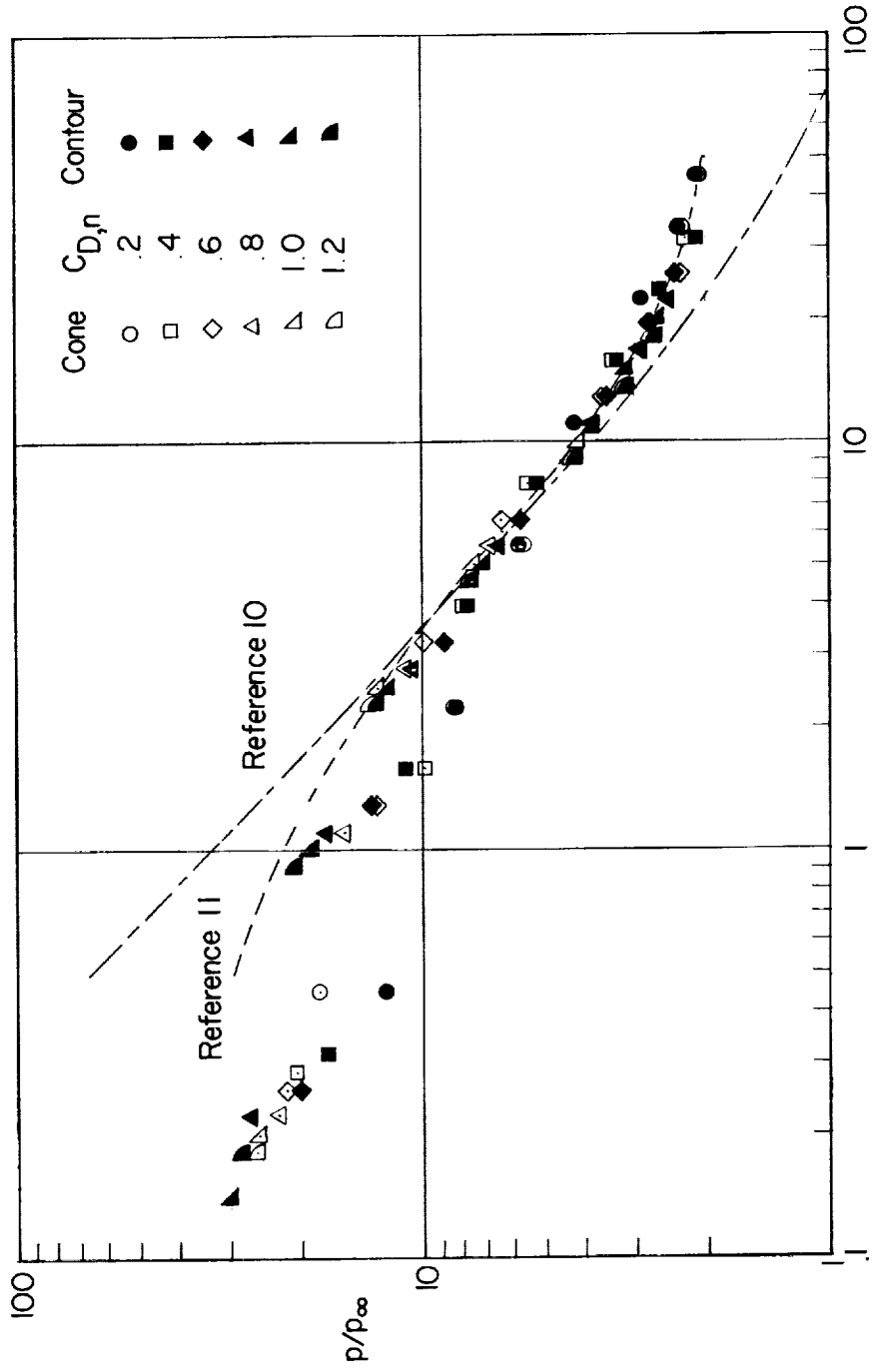

(b) $M_\infty = 21.09$.

Figure 8.- Concluded.

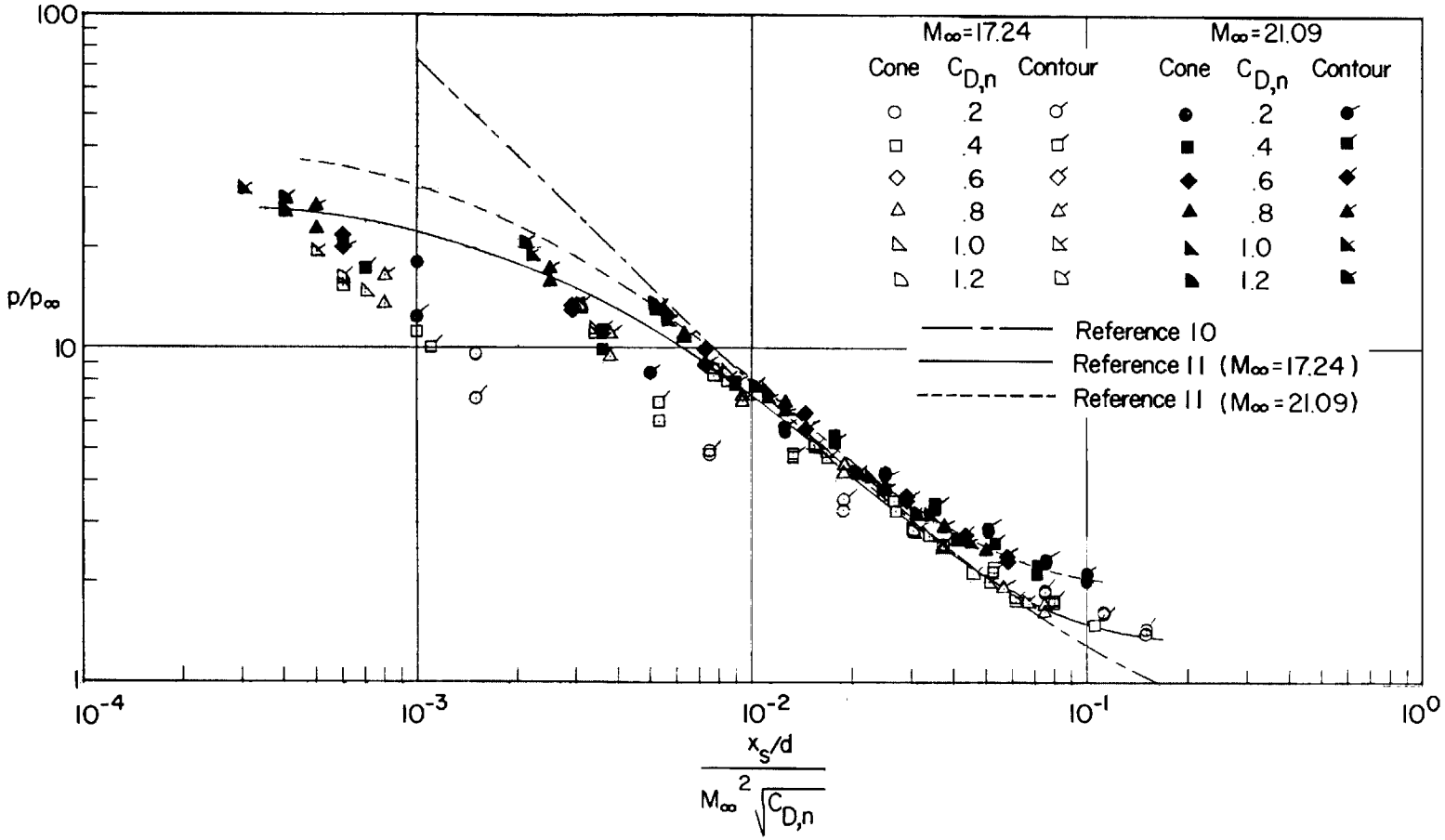

(a) Distance to orifices measured from nose-cylinder juncture.

Figure 9.- Correlation of induced pressures with blast-wave parameter in which Mach number effects are included.

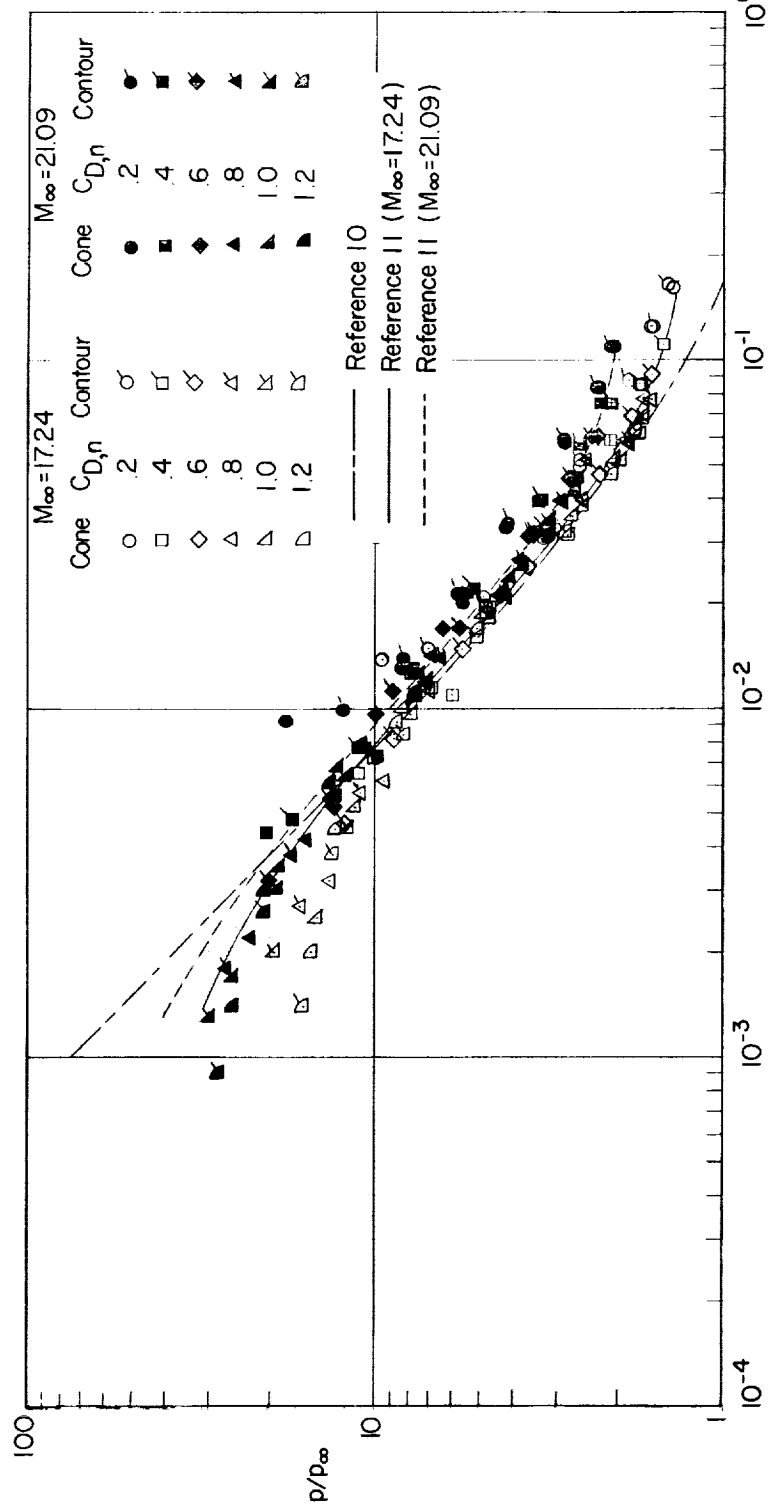

(b) Distance to orifices measured from nose.

Figure 9.- Concluded.

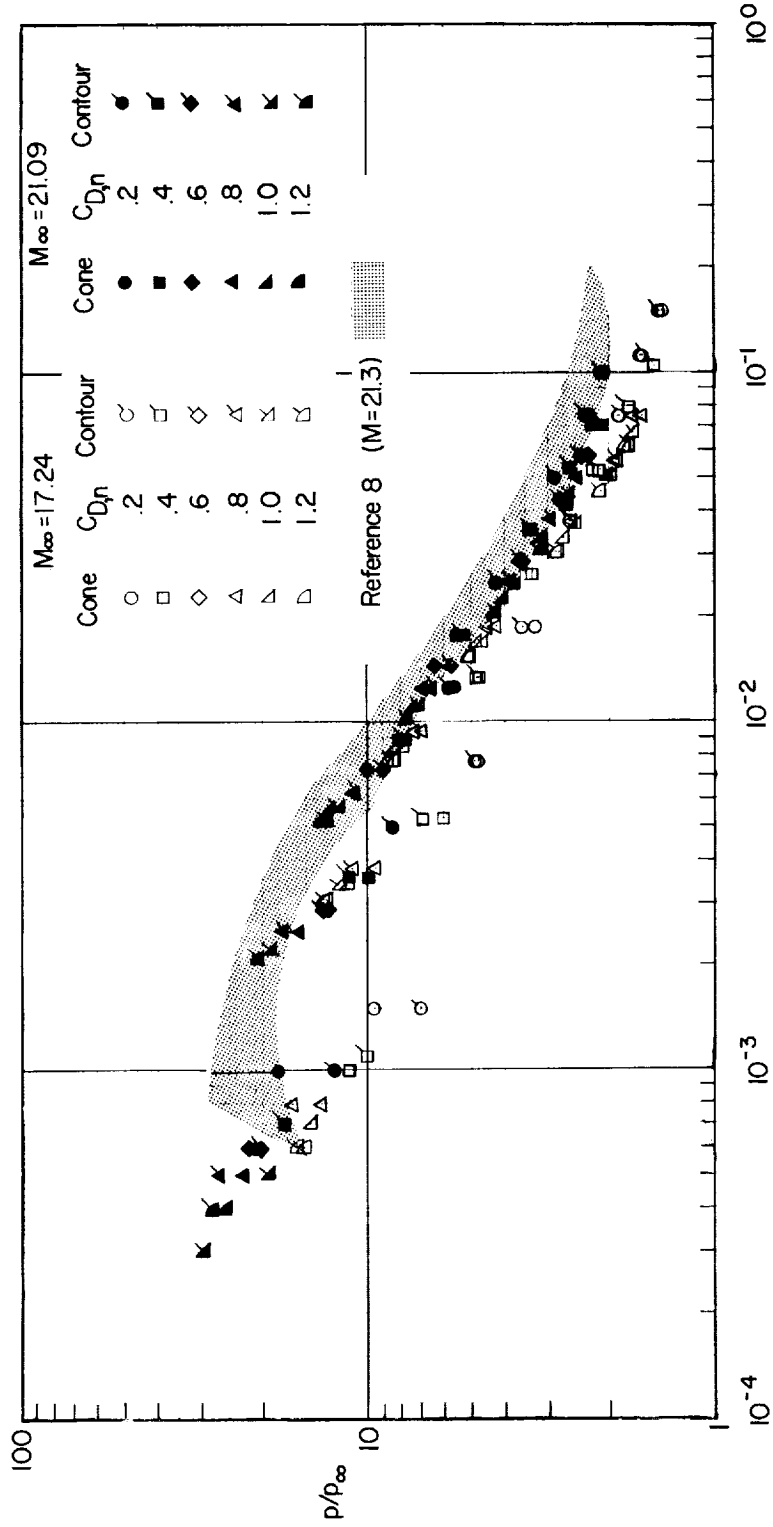

Figure 10.- Comparison of results of the present test with those of a previous investigation.

NASA TN D-1266
National Aeronautics and Space Administration.
INDUCED PRESSURES ON CYLINDRICAL RODS WITH VARIOUS NOSE DRAGS AND NOSE SHAPES AT MACH NUMBERS OF 17 AND 21. Robert D. Witcofski and Arthur Henderson, Jr. May 1962. 35p. OTS price, $1.00.
(NASA TECHNICAL NOTE D-1266)

Six pairs of axially symmetric, flow-alined models were tested at hypersonic speeds in helium. Each pair of models had the same nose-drag coefficient (0.2 to 1.2) but different nose shapes. The induced pressures were found to be functions of nose drag only and independent of nose shape at stations beyond about 1 body diameter downstream of the nose-cylinder junction. "Modified" and "correlated" blast-wave theories adequately predicted induced pressures for only the higher drag models. However, the parameters developed in the theories correlated the data very well, at constant Mach number, for

Copies obtainable from NASA, Washington (over)

I. Witcofski, Robert D.
II. Henderson, Arthur, Jr.
III. NASA TN D-1266

(Initial NASA distribution: 2, Aerodynamics, missiles and space vehicles; 20, Fluid mechanics.)

NASA

NASA TN D-1266
National Aeronautics and Space Administration.
INDUCED PRESSURES ON CYLINDRICAL RODS WITH VARIOUS NOSE DRAGS AND NOSE SHAPES AT MACH NUMBERS OF 17 AND 21. Robert D. Witcofski and Arthur Henderson, Jr. May 1962. 35p. OTS price, $1.00.
(NASA TECHNICAL NOTE D-1266)

Six pairs of axially symmetric, flow-alined models were tested at hypersonic speeds in helium. Each pair of models had the same nose-drag coefficient (0.2 to 1.2) but different nose shapes. The induced pressures were found to be functions of nose drag only and independent of nose shape at stations beyond about 1 body diameter downstream of the nose-cylinder junction. "Modified" and "correlated" blast-wave theories adequately predicted induced pressures for only the higher drag models. However, the parameters developed in the theories correlated the data very well, at constant Mach number, for

Copies obtainable from NASA, Washington (over)

I. Witcofski, Robert D.
II. Henderson, Arthur, Jr.
III. NASA TN D-1266

(Initial NASA distribution: 2, Aerodynamics, missiles and space vehicles; 20, Fluid mechanics.)

NASA

NASA TN D-1266
National Aeronautics and Space Administration.
INDUCED PRESSURES ON CYLINDRICAL RODS WITH VARIOUS NOSE DRAGS AND NOSE SHAPES AT MACH NUMBERS OF 17 AND 21. Robert D. Witcofski and Arthur Henderson, Jr. May 1962. 35p. OTS price, $1.00.
(NASA TECHNICAL NOTE D-1266)

Six pairs of axially symmetric, flow-alined models were tested at hypersonic speeds in helium. Each pair of models had the same nose-drag coefficient (0.2 to 1.2) but different nose shapes. The induced pressures were found to be functions of nose drag only and independent of nose shape at stations beyond about 1 body diameter downstream of the nose-cylinder junction. "Modified" and "correlated" blast-wave theories adequately predicted induced pressures for only the higher drag models. However, the parameters developed in the theories correlated the data very well, at constant Mach number, for

Copies obtainable from NASA, Washington (over)

I. Witcofski, Robert D.
II. Henderson, Arthur, Jr.
III. NASA TN D-1266

(Initial NASA distribution: 2, Aerodynamics, missiles and space vehicles; 20, Fluid mechanics.)

NASA

NASA TN D-1266
National Aeronautics and Space Administration.
INDUCED PRESSURES ON CYLINDRICAL RODS WITH VARIOUS NOSE DRAGS AND NOSE SHAPES AT MACH NUMBERS OF 17 AND 21. Robert D. Witcofski and Arthur Henderson, Jr. May 1962. 35p. OTS price, $1.00.
(NASA TECHNICAL NOTE D-1266)

Six pairs of axially symmetric, flow-alined models were tested at hypersonic speeds in helium. Each pair of models had the same nose-drag coefficient (0.2 to 1.2) but different nose shapes. The induced pressures were found to be functions of nose drag only and independent of nose shape at stations beyond about 1 body diameter downstream of the nose-cylinder junction. "Modified" and "correlated" blast-wave theories adequately predicted induced pressures for only the higher drag models. However, the parameters developed in the theories correlated the data very well, at constant Mach number, for

Copies obtainable from NASA, Washington (over)

I. Witcofski, Robert D.
II. Henderson, Arthur, Jr.
III. NASA TN D-1266

(Initial NASA distribution: 2, Aerodynamics, missiles and space vehicles; 20, Fluid mechanics.)

NASA

NASA TN D-1266

stations beyond 2.5 body diameters from the nose-cylinder junction.

Copies obtainable from NASA, Washington

NASA

NASA TN D-1266

stations beyond 2.5 body diameters from the nose-cylinder junction.

Copies obtainable from NASA, Washington

NASA

NASA TN D-1266

stations beyond 2.5 body diameters from the nose-cylinder junction.

Copies obtainable from NASA, Washington

NASA

NASA TN D-1266

stations beyond 2.5 body diameters from the nose-cylinder junction.

Copies obtainable from NASA, Washington

NASA

NASA TN D-1266
National Aeronautics and Space Administration.
INDUCED PRESSURES ON CYLINDRICAL RODS WITH VARIOUS NOSE DRAGS AND NOSE SHAPES AT MACH NUMBERS OF 17 AND 21. Robert D. Witcofski and Arthur Henderson, Jr. May 1962. 35p. OTS price, $1.00.
(NASA TECHNICAL NOTE D-1266)

Six pairs of axially symmetric, flow-alined models were tested at hypersonic speeds in helium. Each pair of models had the same nose-drag coefficient (0.2 to 1.2) but different nose shapes. The induced pressures were found to be functions of nose drag only and independent of nose shape at stations beyond about 1 body diameter downstream of the nose-cylinder junction. "Modified" and "correlated" blast-wave theories adequately predicted induced pressures for only the higher drag models. However, the parameters developed in the theories correlated the data very well, at constant Mach number, for

Copies obtainable from NASA, Washington (over)

I. Witcofski, Robert D.
II. Henderson, Arthur, Jr.
III. NASA TN D-1266

(Initial NASA distribution: 2, Aerodynamics, missiles and space vehicles; 20, Fluid mechanics.)

NASA

NASA TN D-1266
National Aeronautics and Space Administration.
INDUCED PRESSURES ON CYLINDRICAL RODS WITH VARIOUS NOSE DRAGS AND NOSE SHAPES AT MACH NUMBERS OF 17 AND 21. Robert D. Witcofski and Arthur Henderson, Jr. May 1962. 35p. OTS price, $1.00.
(NASA TECHNICAL NOTE D-1266)

Six pairs of axially symmetric, flow-alined models were tested at hypersonic speeds in helium. Each pair of models had the same nose-drag coefficient (0.2 to 1.2) but different nose shapes. The induced pressures were found to be functions of nose drag only and independent of nose shape at stations beyond about 1 body diameter downstream of the nose-cylinder junction. "Modified" and "correlated" blast-wave theories adequately predicted induced pressures for only the higher drag models. However, the parameters developed in the theories correlated the data very well, at constant Mach number, for

Copies obtainable from NASA, Washington (over)

I. Witcofski, Robert D.
II. Henderson, Arthur, Jr.
III. NASA TN D-1266

(Initial NASA distribution: 2, Aerodynamics, missiles and space vehicles; 20, Fluid mechanics.)

NASA

NASA TN D-1266
National Aeronautics and Space Administration.
INDUCED PRESSURES ON CYLINDRICAL RODS WITH VARIOUS NOSE DRAGS AND NOSE SHAPES AT MACH NUMBERS OF 17 AND 21. Robert D. Witcofski and Arthur Henderson, Jr. May 1962. 35p. OTS price, $1.00.
(NASA TECHNICAL NOTE D-1266)

Six pairs of axially symmetric, flow-alined models were tested at hypersonic speeds in helium. Each pair of models had the same nose-drag coefficient (0.2 to 1.2) but different nose shapes. The induced pressures were found to be functions of nose drag only and independent of nose shape at stations beyond about 1 body diameter downstream of the nose-cylinder junction. "Modified" and "correlated" blast-wave theories adequately predicted induced pressures for only the higher drag models. However, the parameters developed in the theories correlated the data very well, at constant Mach number, for

Copies obtainable from NASA, Washington (over)

I. Witcofski, Robert D.
II. Henderson, Arthur, Jr.
III. NASA TN D-1266

(Initial NASA distribution: 2, Aerodynamics, missiles and space vehicles; 20, Fluid mechanics.)

NASA

NASA TN D-1266
National Aeronautics and Space Administration.
INDUCED PRESSURES ON CYLINDRICAL RODS WITH VARIOUS NOSE DRAGS AND NOSE SHAPES AT MACH NUMBERS OF 17 AND 21. Robert D. Witcofski and Arthur Henderson, Jr. May 1962. 35p. OTS price, $1.00.
(NASA TECHNICAL NOTE D-1266)

Six pairs of axially symmetric, flow-alined models were tested at hypersonic speeds in helium. Each pair of models had the same nose-drag coefficient (0.2 to 1.2) but different nose shapes. The induced pressures were found to be functions of nose drag only and independent of nose shape at stations beyond about 1 body diameter downstream of the nose-cylinder junction. "Modified" and "correlated" blast-wave theories adequately predicted induced pressures for only the higher drag models. However, the parameters developed in the theories correlated the data very well, at constant Mach number, for

Copies obtainable from NASA, Washington (over)

I. Witcofski, Robert D.
II. Henderson, Arthur, Jr.
III. NASA TN D-1266

(Initial NASA distribution: 2, Aerodynamics, missiles and space vehicles; 20, Fluid mechanics.)

NASA

NASA TN D-1266

stations beyond 2.5 body diameters from the nose-cylinder junction.

Copies obtainable from NASA, Washington

NASA